Atomic Spectroscopy

November/December 2018 Volume 39, No. 6

In This Issue:

ASPND7 39(6) 219 – 264 (2018)
ISSN 0195-5373

Atomic Spectroscopy
Vol. 39(6), Nov./Dec. 2018

Printed in the United States and published six times a year by:

PerkinElmer, Inc.
710 Bridgeport Avenue
Shelton, CT 06484-4794 USA
http://www.perkinelmer.com

SUBSCRIPTION INFORMATION
Atomic Spectroscopy
P.O. Box 3674
Barrington, IL 60011 USA
E-mail: atsponline@yahoo.com

2019 SUBSCRIPTION RATES

ORDER ON-LINE:
- pdf only -1 yr - U.S. $60.00
- 2 yr - U.S. $110.00
- pdf and printed copy -
  1 yr - U.S. $90.00
  2 yr - U.S. $160.00
- printed copy only -
  1 yr - U.S. $70.00
  2 yr - U.S. $130.00

PAYMENT BY CHECK:
Check must be drawn on U.S. bank in U.S. funds made out to: "*Atomic Spectroscopy*"

BACK CLAIMS/ADDRESS CHANGES:
- Subscriber claims for missing back issues will be honored at no charge within 90 days of issue mailing date.
  E-mail: atsponline@yahoo.com

ARTICLE INDEXING SERVICES
Thomson Reuters at:
www.scientific.thomsonreuters.com
Elsevier BV at:
www.elsevier.com

Guidelines for Authors

Atomic Spectroscopy serves as a medium for the dissemination of general information together with new applications and analytical data in atomic absorption spectrometry.

The pages of *Atomic Spectroscopy* are open to all workers in the field of atomic spectroscopy. There is no charge for publication of a manuscript.

The journal has around 1100 subscribers on a worldwide basis, and its success can be attributed to the excellent contributions of its authors as well as the technical guidance of its reviewers and the Technical Editors.

The original of the manuscript can be mailed to the editor in hard copy including electronic file on disk or CD (or simply by e-mail) in the following manner:

1. If mailed, provide text (double-spaced) and tables in hard copy plus on disk or CD with text and tables in .doc file; figures in doc or tif files.
3. Number the references in the order they are cited in the text.
5. Consult a current copy of *Atomic Spectroscopy* for format.
6. Editor's e-mail: anneliese.lust@perkinelmer.com or: annelieselust@aol.com

All manuscripts are sent to two reviewers. If there is disagreement, a third reviewer is consulted.

Minor changes in style are made in-house and submitted to the author for approval.

If a revision of the manuscript is required before publication can be considered, the paper is returned to the author(s) with the reviewers' comments.

In the interest of speed of publication, a pdf file of the typeset text is e-mailed to the corresponding author before publication for final approval.

Once the issue has been printed, each author receives a final pdf file of the article including 50 complimentary copies of the article and several copies of the complete issue.

Additional reprints can be purchased, but the request must be made before printing.

PerkinElmer. Inc., holds copyright to all material published in *Atomic Spectroscopy* unless otherwise noted on the first page of the article.

Anneliese Lust
Editor, *Atomic Spectroscopy*
PerkinElmer, Inc.
710 Bridgeport Avenue
Shelton, CT 06484-4794 USA

Trace Metals Screening Process of Devices Used for the Collection, Analysis, and Storage of Biological Specimens

Cynthia D. Ward[a,b], Reba J. Williams[a], Katelyn Mullenix[b], Kristy Syhapanha[b], Robert L. Jones[a], and Kathleen Caldwell[a]

[a] Centers for Disease Control and Prevention, National Center for Environmental Health, Division of Laboratory Sciences, Inorganic & Radiation Analytical Toxicology Branch, 4770 Buford Highway NE MS F-50, Atlanta, GA 30341-3717, USA

[b] Oak Ridge Institute for Science and Education, 4770 Buford Highway NE MS F-50, Atlanta, GA 30341-3717, USA

ABSTRACT

The Centers for Disease Control and Prevention's (CDC) Environmental Health Laboratory uses modified versions of inductively coupled plasma mass spectrometry (ICP-MS) analytical methods to quantify metals contamination present in items that will come into contact with patient samples during the pre-analytical, analytical, and post-analytical stages. This lot screening process allows us to reduce the likelihood of introducing contamination which can lead to falsely elevated results. This is particularly important when looking at biomonitoring levels in humans which tend to be near the limit of detection of many methods. The fundamental requirements for a lot screening program in terms of facilities and processes are presented along with a discussion of sample preparation techniques used for lot screening. The criteria used to evaluate the lot screening data to determine the acceptability of a particular manufacturing lot is presented as well. As a result of lot testing, unsuitable manufactured lots are identified and excluded from use.

INTRODUCTION

Over the last two decades, the Centers for Disease Control and Prevention's (CDC) Inorganic and Radiation Analytical Toxicology Branch (IRATB) has transitioned from using graphite furnace atomic absorption (GFAA) to using inductively coupled plasma mass spectrometry (ICP-MS) to quantify the metal content of various biological matrices. ICP-MS enables accurate quantification of ultra trace levels of numerous toxic and essential metals simultaneously for biomonitoring studies. We also use our analytical methods to assess human exposures to trace, toxic, and essential metals in emergency response situations (i.e., acute exposures) and, as part of biomonitoring studies, for targeted populations of interest. The analytical data from emergency response samples help to determine the specific source of exposure and drive treatment decisions, while data from biomonitoring studies help identify exposures among targeted populations and contribute to national public health policy decisions, and also guide diagnosis and treatment decisions for specific diseases caused by exposure to these metals (1). The data obtained from our laboratory's measurements as part of the National Health and Nutrition Examination Survey (NHANES) are summarized in the National Report on Human Exposure to Environmental Chemicals. In this report, the CDC continuously updates reference levels for the United States population for exposures to various toxic and essential metals of concern (2). The analytical data that our laboratory generates for other biomonitoring studies are used to answer specific questions for targeted populations. Considering the public health significance of these data, it is essential that quality remain a cornerstone of our laboratory's analytical measurements. The quality of our measurements is a reflection of the techniques employed, the skill of our scientists, and the materials used in the process. Seemingly small amounts of contamination could skew analytical results to the point where the perceived patient exposure level can lead to erroneous conclusions, treatment recommendations, and policy decisions (3). The process of lot screening, also referred to as lot testing, enhances the ability to obtain an accurate exposure assessment by minimizing the risk of contamination from sample collection and laboratory devices. Emphasis is typically placed upon the laboratory analyst not introducing errors during the analytical process, but the introduction of contamination during the pre-analytical processes is often overlooked.

In the 1980's, we started incorporating the lot screening process into our analytical systems. We use modified versions of our routine analytical methods to assess the metals content in manufactured lots of materials used for the collection, analysis, and storage of biological specimens undergoing trace metals analyses. We screen manufactured lots for lead (Pb), cadmium (Cd), mercury (Hg), selenium (Se), and manganese (Mn), and also chromium (Cr) and cobalt (Co) when applicable. Serum-related items are screened for zinc (Zn), copper (Cu), and/or selenium.

**Corresponding author.*
E-mail: CWard@cdc.gov
Tel: +1-770-488-7302
Fax: +1-770-488-0509

Items related to the collection, analysis, and storage of urine samples are screened for the following metals: antimony (Sb), arsenic (As), barium (Ba), beryllium (Be), cadmium, cesium (Cs), chromium, cobalt, iodine (I), lead (Pb), molybdenum (Mo), manganese, mercury, nickel (Ni), platinum (Pt), strontium (Sr), thallium (Tl), tin (Sn), tungsten (W), and uranium (U) (4, 5). Analytes such as lead, barium, and manganese are more problematic than others. Using materials that have metals concentrations below thresholds defined by our biomonitoring requirements provides assurance that the analytical results obtained are indeed a result of the patient specimen itself and are not falsely elevated because of contamination from items used in the collection and analytical process.

Our lot screening efforts have evolved over the years. CDC scientists currently use inductively coupled plasma mass spectrometry (ICP-MS) and modified versions of our routine analytical methods for biological specimens to determine the amount of metals contamination present in items that will come into contact with patient samples during the pre-analytical, analytical, and post-analytical stages. In 2005, we established a dedicated laboratory to focus solely on lot screening analyses. Between 2002 and the present, IRATB has seen an increase in both the number of items screened and the analytical methods utilized within our laboratory. The literature contains a few references to the concept of lot screening, but our laboratory provides a comprehensive, dedicated lot screening program geared towards all aspects of the analytical process: sample collection, processing, sample analysis and handling within the laboratory, and sample storage (6). The process utilized is explained in this manuscript. A discussion of lot screening results obtained over a 14-year time period is provided as well. The results obtained validate the necessity of performing lot testing to obtain accurate measurements that are not biased due to contamination.

EXPERIMENTAL

Background

We perform lot screening analyses on manufactured lots of materials purchased for use in our laboratory and for use in field studies, including materials used for CDC's blood metals, serum, and urine methods. We also screen materials purchased directly by our collaborators for large studies such as NHANES when the biological specimens will be submitted to our laboratory for metals analysis. An alternative to lot screening would be to acid wash devices or containers before use; however, the high sample throughput for our analytical methods eliminates the practicality of acid washing individual items. Acid washing is not feasible for all types of devices and containers for a number of reasons. For items that can be acid washed, the process is too time-consuming considering the workflow within the laboratory. Other items, such as evacuated blood and serum tubes cannot be acid washed because the vacuum would have to be broken to do so. Additionally, devices that contain anti-coagulants and preservatives cannot be acid washed because acid washing would remove the anti-coagulant or preservative.

Potential sources of metals contamination introduced during manufacturing processes include materials used to make the devices (glass, stainless steel, rubber, or plastic), colorants, preservatives used in collection devices, and the manufacturing machinery. The conditions of the manufacturing processes involved in the production of commercial devices can differ with each batch (or "lot") of materials produced; therefore, the amount of contamination introduced can vary from lot to lot making it necessary to test materials from each manufactured lot that will be used in the analytical process.

Requirements for a Lot Screening Program

We have identified four fundamental laboratory requirements that need to be in place prior to implementation of an effective metals lot screening program. First, the laboratory needs to have analytical methods developed and implemented that allow the analysts to measure ultra trace concentrations of the metals of concern in aqueous solutions. Second, the laboratory needs to have access to a "clean" environment. Devices should be prepared for testing inside of a laminar flow hood Class 100 or better to reduce the likelihood of exposure to external contamination of the items being screened. The third requirement is precautionary measures that ensure analysts performing lot testing are not introducing contamination into the process. These measures include, but are not limited to, using clean powder-free gloves to handle the devices, minimizing the handling of the devices to be screened, ensuring that reagents used in the process are free from contaminants, and ensuring that clean metals-free equipment is used throughout the steps of the screening process. The fourth requirement is having a system in place to evaluate and track the results. Our screening program exceeds these four requirements. Our laboratory uses a dedicated clean room for lot testing. The room falls under ISO 14644-1 class ISO 6 which is equivalent to the FED STE 209E class 1,000 designation (7). We use class II type A2 biological safety cabinets within this room to prepare samples in. All analytical instruments and

equipment used are dedicated to lot screening; the lot screening instrumentation and equipment is never exposed to biological matrices. In addition to focusing on the fundamentals, we periodically evaluate the analytical methods used to assess efficiency and best practices. We use extensive preventative maintenance and cleaning protocols to maintain all lot screening analytical instruments and equipment. All reagents are prepared in acid-washed containers that have been thoroughly rinsed with ≥18 MΩ-cm deionized water. Rinsate from the cleaned containers is analyzed to ensure that residual contamination is not present after cleaning. The reagents used and solutions made are screened using the ICP-MS to ensure that they are not contaminated. For this screening, we analyze a dilution of the reagent or the solution itself to compare the counts per second obtained to those of a blank or deionized water. If reagents have analytes present at levels higher than we typically see in our reagent blanks, we seek alternate sources for the reagents.

Lot Screening Process

Our laboratory maintains a supply of pre-screened materials on hand for use in field studies and emergency response situations. We evaluate manufactured lots of vacuum-sealed evacuated blood tubes, vacuum-sealed serum tubes, needles (18G, 21G, 23G, and 25G), luer adapters, syringes, cryogenic vials, centrifuge tubes, urine collection cups, pediatric urine collection bags, disposable transfer pipets, pipette tips, alcohol pads and wipes, among other items. Our preference is to provide our pre-screened materials, whenever possible, to eliminate possible bias in analytical results from our external collaborators using contaminated specimen collection materials. When collaborators purchase their own materials for use, we ask that they send a portion of each manufacturing lot to our laboratory for screening prior to sample collection. We provide standardized request forms to each entity requesting screening services to ensure that pertinent information is captured for each manufactured lot. From every manufactured lot, our laboratory screens 50 units, ensuring that no more than 5% of the units can be expected to be defective in an acceptable lot with a 90% confidence. The basis for testing 50 units from each lot was statistically derived (8). First, a screening solution is tested for the analytes of interest, and only a solution that is known not to have analyte concentrations above the analytical method limits of detection is used in the screening process. The screening solution is then added to or passed through laboratory devices, and the solution is subsequently tested to determine if the analytes of interest are present. If the analysis of the solution after contact with the device shows the presence of contamination at levels that are unacceptable, the lot is deemed unsuitable and is not used.

Some laboratory consumables, such as storage vials and collection devices, come with certifications from the manufacturers about their metals content. Only specific metals are tested, so data for all of our analytes of concern is not available. Another problem with the vendor-provided certifications is that the levels at which these items are certified is significantly higher than the low parts per billion (ppb) and parts per trillion (ppt) levels that are of concern with biomonitoring measurements. In most instances, these vendor-provided certifications are based on the United States' Pharmacopeia (USP) <231> for heavy metals which is qualitative in nature. For example, a specific brand of centrifuge tube that is designated "metal-free" has a statement of the certificate of quality for each lot that the bulk material used to make the centrifuge tubes had heavy metals concentrations less than 1 ppb. When you are using methods with detection limits 10 or 100 times lower than 1 µg/L, this is problematic. Other manufacturing process-related factors to consider in addition to the metals content of the bulk materials are cleanliness of the machinery used to make the equipment (stainless steel components can lead to contamination), the cleanliness of the manufacturing environment (airborne metal contaminants that may settle on the product being manufactured), and metal contamination levels of other products made within the same manufacturing environment. All of these factors along with others have an impact on the resulting metals concentrations in the final manufactured product. USP 231, which was scheduled to be deleted at the beginning of 2018, has been replaced with quantitative methods USP <232> and USP <233> (9). This was a step in the right direction; however, it still did not address the specific problems that we experience with materials not being suitable for our biomonitoring measurements.

Instrumentation

Our laboratory uses a PerkinElmer® ELAN® Dynamic Reaction Cell™ (DRC™) II ICP-MS (PerkinElmer, Inc., Shelton, CT, USA) for screening of devices used for blood metals analysis, serum metals analysis, and the analysis of iodine and mercury in urine. We use a PerkinElmer NexION® 300D ICP-MS with Universal Cell Technology™ (UCT™) and DRC capabilities for screening of the remaining urine metals. Both ICP-MS instruments used currently are equipped with nickel sampler and skimmer cones, a 2.0-mm quartz injector, and a quartz cyclonic spray cham-

ber. The instrument parameters are listed in Table I. We use a SC4-DX FAST autosampler (Elemental Scientific Inc., Omaha, NE, USA) with both instruments. We use >99.999% argon for the plasma gas. Our laboratory's use of DRC gases mirrors what is used in the actual analytical method used to analyze patient samples. We use methane and oxygen as DRC gases during the analysis of items screened for blood metals analysis, while we use ammonia as a DRC gas during testing of items screened for serum metals analysis (4, 5). For the urine metals screening, the ICP-MS is operated in vented mode.

Sample Preparation and Analysis

To determine the suitability of different devices for sample collection, preparation, analysis, and storage, we test an aliquot of screening solution that has been exposed to the surfaces of the device that will be exposed to a patient sample. The screening solution is typically a dilute acidic solution (0.5% nitric acid) or deionized water. Once the devices are received in-house for screening, scientists in the lot screening laboratory add the appropriate amount of lot screening solution to each of the 50 units. Either we pass a screening solution through the device (e.g., needles, pipette tips), or we put screening solution in the device (e.g., urine cups and cryogenic vials) and subsequently prepare an aliquot of the solution for analysis. The contact time of the solution with each unit

TABLE I
ICP-MS Instrumental Parameters for Screening Methods

Parameters	Settings Used[a]		
ICP-MS	Urine Multielement	Serum	Blood
RF Power	1450 W[a] (ELAN) 1600 W[a] (NexION)	1450 W[a] (ELAN)	1450 W[a] (ELAN)
Plasma Gas Flow	15 L/min[a]	15 L/min[a]	15 L/min[a]
Auxillary Gas Flow	1.2 L/min[a]	1.2 L/min[a]	1.2 L/min[a]
Nebulizer Gas Flow	~ 0.9-1.01 L/min[a]	~ 0.8-1.00 L/min[a]	~ 0.9-1.0 L/min[a]
Sweeps/Reading	40	90	30
Readings/Replicate	1	1	1
DRC Channel Gas A		0.5 L/min	0.84 (Se)
DRC Channel Gas B			1.2 (Mn, Hg)
Number of Replicates	3	3	3
RPq	0.25	0.7	0.6 (Mn, Hg) 0.65 (Se) 0.25 (Cd, Pb
RPa	0	0	0
Dwell Time	30 ms (Co, Sr, Mo, Rh, Cd, Sn, Sb, Cs, Mn, Ba, W, Ir, Tl, Pb) 100ms (Pt, U)	30 ms (Zn, Cu, Se)	50 ms (Rh, Te, Te-1, Ir) 100 ms (Mn, Hg, Se, Pb) 150 ms (Cd)
Scan Mode	Peak Hopping	Peak Hopping	Peak Hopping
Detector Mode	Dual	Pulse	Dual
Analytes Tested	Be, Co, Sr, Mo, Cd, Sb, Cs, Sn, Ba, Mn, W, Pt, Tl, Pb, U, As	Zn, Cu, Se	Mn, Hg, Se, Cd, Pb
Sampling			
Sample Flush	11 s, -3 rpm	35 s, -15 rpm	6 s, -5 rpm
Read Delay	45 s -3 rpm	45 s, -15 rpm	60 s, -5 rpm
Analysis	-3 rpm	-15 rpm	-5 rpm
Wash	50 s, -3rpm	30 s, -15 rpm	40 sec, -5 rpm

[a] Suggested starting values only. Optimum parameters will depend on outcome of the optimization procedure and the instrument being used.

differs based on the type of device being screened. For example, with needles we pass the screening solution through the needle into a prescreened evacuated blood tube. The contact time with the screening solution is identical to the contact time of blood being passed through a needle. To yield 50 specimens, we repeat the process for 49 additional needles from the same manufactured lot. For cryogenic vials, we uncap the vials, add screening solution, and recap the vial. We invert the 25 odd-numbered cryogenic vials and let the devices sit overnight. This process allows us to determine if contamination, if present, is coming from the vial (the even units that were left upright), the cap (all of the inverted vials), or both. Multiple types of devices are assessed in this manner. We determined that 8 to 12 hours is more than enough time to get surface contamination, if present, in solution.

We prepare aliquots for analysis through simple dilution methods using a Hamilton® Microlab® 625® Advanced Dual Syringe diluter (Hamilton Company, Reno, NV, USA) equipped with a 5-mL dispensing syringe and a 1,000-µL sampling syringe. Electronic single-channel pipettes are used for intermediate calibrator stock preparation, and a 5-place analytical balance is used to weigh out solid reagents. We take an aliquot of the solution from each of the 50 units and dilute it with diluent using the same ratio that would be used for a patient sample. We prepare a matrix blank by diluting a screening solution that is stored in prescreened containers. To preserve the correlation between the associated analytical methods used for biological specimens, we make certain that each screening analytical method is as close to the actual analytical method as possible. The reagents are prepared in a similar fashion with the exception of being prepared in water instead of the corresponding biological matrix. The preparation specifics for the solutions and controls used in these methods are listed in Table II.

Within the same analytical run, we analyze quality control materials to demonstrate the acceptability of instrument performance and to confirm the proper preparation of samples. We treat the prepared aliquots from each of the 50 units in each manufactured lot as unknowns, allowing us to quantify the metals content, if any, present in the solution. We prepare quality control materials from different lots of materials than the lots used for the preparation of calibrators. A ±10% recovery limit is used for the pass/fail determination of the quality control materials used within the analytical run. If the QC materials are not within limits, the analytical run has to be repeated.

Historically, our laboratory utilized several different screening solutions. Initially, we used aqueous solutions that had the same chemical constituents as the diluents used in the methods used to analyze patient samples in the matrix of interest. We simplified the process by using a dilute acidic solution for everything, and over time, we further simplified processes by using 0.5% nitric acid as the screening solution for all analytical methods regardless of the patient sample matrix. We found that the dilute acidic solution effectively mimicked the solubility characteristics of patient samples. The screening solution, rinses, diluents, and calibrators are prepared using double-distilled concentrated (68%-70%) nitric acid. Each bottle of double-distilled nitric acid is tested before the screening solutions, instrument rinses, and sample dilu-

TABLE II
Solutions and Calibration Standards Used in the Screening Methods for Each Matrix

Screening Method	Rinse Composition	Diluent Composition	Quality Control Materials	Volume of Sample: Diluent in µL
Blood Metals	0.1% APCD[a], 0.05% Triton-X®, 0.4% TMAH[b], 1% EtOH in DI H_2O	5 µg/L Rh[d], Ir[e], Te[f] in 0.01% APCD[a], 0.05% Triton-X®, 0.4% TMAH[b], 1% EtOH in DI H_2O	Calibration Standard 2 IV QC[g]	200:4800
Serum Metals	2% HNO_3[c] in DI H_2O	10 µg/L Ga[h] in 0.5% HNO_3[c] in DI H_2O	Standard 2 SRM 1640a[i]	300:4200
Urine Metals	2% HNO_3[c] in DI H_2O	10 µg/L Ga[h], Rh[d], Ir[e] in 2% HNO_3[c] in DI H_2O	Standard 2 IV QC	200:4800

[a] Ammonium pyrrolidine dithiocarbamate. [b] Tetramethylammonium hydroxide. [c] Nitric acid. [d] Rhodium. [e] Iridium. [f] Tellurium. [g] Inorganic Ventures quality control material. [h] Gallium. [i] National Institute for Standards and Technology 1640a.

ent are prepared to ensure that contamination is not being introduced with the reagents being used. In addition to testing the nitric acid used in the screening process, we test all reagents used by evaluating the counts per second obtained with each analyte when screened using the ICP-MS. Any reagent with evidence of potential contamination is not used. We also use different lots of reagents to account for variations in the analytical process.

During a period of evaluation of the current lot screening processes, we implemented a change to our typical screening approach. With metallic components such as stainless steel needles, we now use deionized water instead of 0.5% nitric acid as the screening solution. The reason for that change was to eliminate metal contamination that we attributed to leaching of metals out of the stainless steel needle that would not be leached out during the short period of contact between the blood and the needle. Additionally, since the normal pH of blood is between 7.36 and 7.41, the pH of water more closely resembles blood than our 0.5% nitric acid screening solution which has a pH of approximately 1.3 (10). Based on this information, we implemented use of deionized water as the screening solution for all blood-metals related devices.

RESULTS AND DISCUSSION

Evaluation of Lot Screening Data

The analytical results for the analysis of aliquots from a specific manufactured lot are not the only determining factor of the acceptability of a manufactured lot of materials. Our laboratory uses the following information to determine the acceptability of a specific lot for each individual analyte of interest: the limit of detection (LOD) of the biomonitoring methods, expected population mean, the typical sample volume that is collected in the device (or the known specific volume that will be used for a particular study), the amount of screening solution used when setting up the device, and the analytical results obtained via screening. The LOD is the lowest value that can be tested for a particular analyte with certainty when applying the normal analytical method for patient samples. The LODs for the analytical methods used for patient samples are derived from the analysis of matrix-matched calibration standards over at least 60 runs. The method used to calculate LODs in our laboratory is a standardized process defined by the Division of Laboratory Sciences. It accounts for both Type I and Type II errors. We use the patient sample analytical method LODs for the screening methods under the assumption that the screening LOD is lower than the LOD of the analytical method because the screening methods are aqueous and there is no matrix present.

Any screening result obtained that is greater than the LOD is logged into a spreadsheet used to report results. The expected population mean is the expected mean concentration of the analyte of interest in the population to be studied. This data is available in the most recent version of the *National Report on Human Exposure to Environmental Chemicals*. The values are updated with each release of NHANES data. For newer methods where NHANES data are not available, we rely on available reference values from the literature. In instances where neither NHANES nor reference values are available, we analyze a number of patient samples via that method and calculate the mean values in that subset. The volume of sample in a device is the amount of patient sample that is either going to pass through the device or be stored in the container tested and is determined by the requestor. We give guidance to the requestors to ensure that the screening results provided reflect the intended usage of the device. Table III lists the guidelines for determining the amount of sample that the end user expects will be exposed to the device. The volume of screening solution is the amount of screening solution that passes through the devices or is aliquotted in the storage container during screening.

The presence of some levels of the analyte does not necessarily mean that the device is unsuitable for use. The maximum allowable contribution is the maximum total concentration of the analyte that can be present in the device or container and still be deemed acceptable for use. It is determined using some of the previously described factors with the following equation:

$$\text{Max Allowable Contribution} = \frac{(\text{Expected Population Mean}) \times (\text{Max \% Contribution}) \times (\text{Volume Sample in Device})}{(\text{Volume Screening Solution})}$$

The maximum percent contribution describes the percentage of the analyte that is allowed to be present in the device tested. We set this at a default value of 10%. If the calculated maximum allowable contribution is less than the LOD for the analytical method used for patient samples, then the maximum allowable contribution defaults to 1.5 times the LOD of the method.

A lot is deemed a failure if the result for any particular analyte for multiple units is above the maximum allowable contribution. If only one unit of the 50 screened fails in a lot, the laboratory supervisor can decide whether this failure should be considered an outlier. This determination is based upon specific knowledge of the analyte, such as whether it is one that we can reasonably find in the laboratory (i.e., if random contamination is possible). If the failure is deemed an outlier, the lot is identified as

suitable for use. However, if multiple units have concentrations above the LOD in addition to one unit having a concentration above the maximum allowable contribution, the manufactured lot is marked as failing for the affected analyte(s). If no devices are above the maximum allowable contribution, we consider the lot acceptable for use by the methods tested and the analytes evaluated.

Table IV shows the number of manufactured lots of materials screened by our laboratory per NHANES cycle. The data are broken down by device type and sample matrix. In this manuscript, we provide data as early as 2001; however, the 2009–2010 NHANES cycle was the first one where we screened devices for the complete panel of metals that we currently measure. When calculating the percentage of failures screened per analyte, we take into consideration the number of lots actually tested for that analyte. For example, if we tested 10 lots during a NHANES cycle but only 5 of the lots were tested for zinc, the percentage of failures would be based solely on the 5 lots tested for zinc.

Serum Metals

Between 2002 and 2016, our laboratory screened 365 manufactured lots of materials for Zn, Cu, and/or Se to support our serum metals analyses. As shown in Table V, background contamination in the devices was as high as 1408 µg/L for zinc in an alcohol prep pad. The 387 µg/L failure was from an EDTA-containing evacuated blood tube while the 204 µg/L failure was from a 0.25 mL microcentrifuge tube. To put this in perspective in terms of biomonitoring, the geometric mean of zinc in the U.S. population according to the 2013-2014 cycle of NHANES data was 80.4 µg/L. The three highest copper failures were from needles and cryovials, and the selenium failures were from a manufactured lot of needles. While the geometric means for copper and selenium in the U.S. population for the 2013-2014 NHANES cycle were 115 µg/L and 128 µg/L, respectively the LODs were 2.5 µg/L and 4.5 µg/L, respectively.

Urine Metals

Between 2002 and 2016, our laboratory screened 404 manufactured lots of materials for the urine metals which include As, Ba, Be, Cd, Cs, Co, Pb, Mn, Mo, Pt, Sr, Tl, Sb, Sn, W, and U. The highest screening results from the individual lots screened from 2002 through 2016 are shown in Table VI for each analyte. In nearly all cases, the failures were higher than the NHANES geometric mean for the U.S. population and the method LOD for each analyte; in most cases significantly higher. The two highest failures for barium are from two separate lots of wipes. It should be noted that there were multiple failures within each of these lots. The highest failures for antimony and manganese were also from screened lots of wipes. The elevated lead failures were from urine cups. Overall, the highest failures shown were from a wide array of types of devices – centrifuge tubes, urine cups, wipes, cryovials, pipette tips, and urine bags. In terms of all failures seen, there were failures across all the types of devices that have been

TABLE III
Volume of Patient Sample Expected to Come Into Contact With Different Types of Devices

Type of Device	Typical Specimen Volume	Reasoning
Evacuated blood and serum tubes and micro-collection vials	Full volume of the collection device	The full volume will be drawn due to the vacuum
Cryogenic vials	Smallest volume that you expect the vials will contain	Provides a more conservative estimate
Gauze and alcohol prep pads	Volume of blood expected to be collected in the capillary blood collection procedure	Use of the smallest volume to get the most conservative estimate of the effect of contribution
Syringes and transfer pipettes	Half of the full volume of the syringe	Used for a wide array of volumes – provides a conservastive estimate
Needles and luer adapters	Full volume of the smallest blood tube that would be used	The full volume will be drawn due to the vacuum
Collection cups and centrifuge tubes	Half of the maximum volume unless a specific volume is known	Provides a more conservative estimate
Lancets	Volume of blood expected to be collected in the capillary blood collection procedure	

TABLE IV
The Number of Manufactured Lots Screened for Each Type of Device for Each Matrix During the NHANES Cycle Years from 2001 Through 2016

Sample Type	Type of Device	NHANES Cycle Years							
		2001-2002	2003-2004	2005-2006	2007-2008	2009-2010	2011-2012	2013-2014	2015-2016
Urine									
	Transfer pipettes		1	1		4	6	20	5
	Cryogenic vials	2	1	5	8	8	25	48	39
	Pipette tips		1			2	14	13	8
	Urine cups	4	4	2	9	9	9	28	28
	Centrifuge tubes	3	4	2	3	2	6	12	11
	Syringes					8		1	4
	Bags					1	2	8	2
	Wipes						1	2	11
	Miscellaneous				1	8	3	2	3
Blood									
	Alcohol pads	1	5	3	1		2	2	2
	Blood bags					7	1		
	Centrifuge tubes		1		3	4	2	3	4
	Cryogenic vials	3	3	3	2	5	5	15	15
	Lancets			4		4			5
	Luer adapters		4	4	3	4	1	1	7
	Miscellaneous					8	5	2	3
	Needles		8	17	21	35	11	42	30
	Pipette tips					4	5	2	1
	Pipettes		1	1		2	4	13	2
	Syringes		2	4		7	1	7	3
	Evacuated blood tubes	5	19	15	9	27	13	41	34
Serum									
	Needles		3	7	8	20	10	41	30
	Lancets			2		2			
	Luer adapters					1	1	1	8
	Alcohol pads		2	1			2	2	
	Transfer pipettes		1	1		2	4	13	2
	Centrifuge tubes	1	1		2	3	3	3	5
	Pipette tips						3		4
	Cryogenic vials	2	1	4	3	6	10	22	21
	Syringes		1	6				7	4
	Evacuated serum tubes	4	3	7	5	11	14	17	17
	Miscellaneous	1					2	2	6
	Total	26	66	89	78	194	165	370	314

TABLE V
Screening Data for Serum Metals 2002-2016 – Highest Failures

Metal	Highest Failure (µg/L)	2nd Highest Failure (µg/L)	3rd Highest Failure (µg/L)	2013-2014 NHANES Geometric Mean (µg/L)	LOD[a]
Zinc	1410	387	204	80.4	2.9
Copper	8.49	17.1	14.0	115	2.5
Selenium	25.4	23	N/A	128	4.5

[a]This LOD was used during the 2013 to 2014 NHANES cycle.

TABLE VI
Screening Data for Urine Metals 2002-2016 – Highest Failures

Metal	Highest Failure (µg/L)	2nd Highest Failure (µg/L)	3rd Highest Failure (µg/L)	2013-2014 NHANES Geometric Mean (µg/L)	LOD[a]
Antimony	125	98.6	30.1	0.043	0.022
Arsenic	17.2	7.14	2.15	6.29	0.26
Barium	2170	157	84.1	1.09	0.06
Beryllium	2.66	2.6	0.331	[b]	0.072
Cadmium	15.2	4.2	0.636	0.124	0.036
Cesium	6.03	N/A	N/A	3.94	0.086
Cobalt	9.92	7.29	4.38	0.391	0.023
Lead	96.4	64.8	64.8	0.277	0.03
Manganese	169	157	77.1	[b]	0.13
Molybdenum	1.40	0.971	N/A	33.9	0.8
Platinum	0.701	0.265	0.18	[b]	0.009[c]
Strontium	237	174	153	81.2	2.34
Thallium	0.992	0.212	0.067	0.141	0.018
Tin	9.26	8.92	4.36	0.433	0.09
Tungsten	1.35	0.413	0.41	0.059	0.018
Uranium	0.164	0.135	0.12	0.005	0.002

[a] The LOD is the one used during the 2013 to 2014 NHANES cycle.
[b] The geometric mean was not calculated due to an insufficient number of results above the limit of detection.
[c] The LOD for platinum was from the 2009-2010 NHANES cycle.

screened for urine metals across the years. Urine devices are also screened for mercury and iodine when needed, but we have rarely seen failures for those metals over the years. Chromium and nickel are two recent additions to the urine metals screening panel; however, they were not discussed due to insufficient data.

Blood Metals

Between 2002 and 2016, our laboratory screened 533 manufactured lots of materials for Mn, Hg, Cd, Se, and/or Pb to support our blood metals analyses. Background contamination for manganese in the lots screened was as high as 924 µg/L in one screened lot of needles, while the second and third highest failures were from cryovials and gauze pads. The two mercury failures were from a manufactured lot of pipette tips and one lot of transfer pipettes. The 62.1 µg/L selenium failure was from a transfer pipette. All of the cadmium failures were from one specific lot of gauze pads, while the lead failures were from EDTA-containing evacuated blood tubes, vials, and alcohol prep pads. All of the failures listed in Table VII were above the laboratory LOD for these metals, and all except selenium were also above the geometric means for U.S. population for the 2015 to 2016 NHANES cycle.

CONCLUSION

Testing a representative sample of each manufactured lot (50 items from each lot) can detect contamination that would significantly

TABLE VII
Screening Data for Blood Metals 2002-2016 – Highest Failures

Metal	Highest Failure (µg/L)	2nd Highest Failure (µg/L)	3rd Highest Failure (µg/L)	2015-2016 NHANES Geometric Mean (µg/L)	LOD
Manganese	924	180	74.8	9.59	0.99
Mercury	0.465	0.35	N/A	0.678	0.28
Selenium	62.1	N/A	N/A	191	24.5
Cadmium	1.33	1.25	1.19	0.238	0.1
Lead	20.9[a]	12.7[a]	6.98[a]	0.820[a]	0.07[a]

[a]Lead is in µg/dL.

affect the analytical results obtained from using the materials. Our laboratory has generated over 15 years of data that validate the necessity to continue lot screening efforts. Contamination is spurious enough to validate the need for screening all manufactured lots used in the lab. Using contaminated supplies for collection or analysis has a trickle-down effect on the entire analytical process. Contamination at any point in the process produces falsely elevated patient results, leading to incorrect reference range determinations with biomonitoring data. These incorrect ranges can result in invalid assumptions. In instances where untested devices are used in either the collection, sample processing, analytical processing, or storage, any elevated results could be due to contamination and may not be truly representative of the patient samples. If contamination is identified in collection materials after analytical results have already been obtained, the results will be invalidated; therefore, it is imperative that screening is performed prior to items being used at any step of the analytical process: sample collection, sample analysis, or sample storage.

Conflicts of Interest:

The authors (Cynthia D. Ward, Reba J. Williams, Katelyn Mullenix, Kristy Syhapanha, Robert L. Jones, and Kathleen Caldwell) have no conflicts of interest relevant to this article to disclose.

Received May 24, 2018.

REFERENCES

1. R. Y. Wang, K. L. Caldwell, and R. L. Jones, J. Med. Toxicol. 10, 232 (2014).
2. Centers for Disease Control and Prevention. Fourth Report on Human Exposure to Environmental Chemicals, Updated Tables (March 2018) Atlanta, GA: U.S. Department of Health and Human Services, Centers for Disease Control and Prevention.
3. K. L. Caldwell, P. Y. Cheng, J. M. Jarrett, A. Makhmudov, K. Vance, C. D. Ward, R. L. Jones, and M. E. Mortensen, Pediatrics, 140(2): e20170272 (2017).
4. J. M. Jarrett, R. L. Jones, K. L. Caldwell, and C. P. Verdon, At. Spectrosc. 28(4), 113 (2007).
5. D. R. Jones, J. M. Jarrett, D. S. Tevis, M. Franklin, N. J. Mullinix, K. L. Wallon, C. D. Quarles, K. L. Caldwell, and R. L. Jones, Talanta 162, 114 (2017).
6. I. Rodushkin and F. Odman. J. Trace Elem. Med. Biol. 15, 40 (2001).
7. Clean Air Technology, Inc., What is a Cleanroom? (2017). http://www.cleanairtechnology.com/cleanroom-classifications-class.php. (Accessed 11 Nov. 2017.)
8. W. D. Johnson, Biostatistics, Reinhold Publishing Corporation (1966).
9. K. Zaidi, USP chapters <232> and <233> implementation strategy PowerPoint presentation. https://www.fda.gov/downloads/Drugs/NewsEvents/UCM517456.pdf. (Accessed 11 Oct 2017.)
10. J. B. Henry, Clinical diagnosis and management by laboratory methods, 17th edition, W.B. Saunders Company (1984).

Enrichment of Some Heavy Metals With Cloud Point Extraction via 5,7-Diiodo-8-Hydroxyquinoline Ligand and Detection by Ultrasonic Nebulizer-ICP-OES Using Internal Standard Method

Mustafa Sahin Dundar*, Ferhat Kaptan, Celal Caner, and Huseyin Altundag
Sakarya University, Faculty of Arts and Sciences, Department of Chemistry, 54187 Sakarya, Turkey

ABSTRACT

In this study, a method was developed in which the heavy metal ions of Cu^{+2}, Cd^{+2}, Co^{+2}, Ni^{+2}, Pb^{+2}, Zn^{+2} in water samples are enriched by using cloud point extraction and detection using ultrasonic nebulization with inductively coupled plasma optical emission spectrometry (USN-ICP-OES). The metal ions, complexed with the Triton X-114 surfactant, were imprisoned in the mycelium after phase separation via the centrifuge. The surfactant phase was diluted with 2 M HNO_3 and measured by USN-ICP-OES. In order to reduce noise and errors, indium was used as the internal standard. The pH, surfactant concentration, ligand concentration, equilibration time, temperature, and foreign ion effects were investigated. The limit of detection of Cu^{+2}, Zn^{+2}, Ni^{+2}, Cd^{+2}, Co^{+2}, Pb^{+2} usingt pH=7, 0.1 mmol L^{-1} 5,7-diiodo-8-hydroxyquinoline, and %0.06 (w/v) Triton X-114 were found to be 0.076, 0.30, 0,081, 0.022, 0.033, and 0.049 µg L^{-1}, respectively. The RSD% was between 2.08% and 6.28% (n=10). The developed method is in accordance within green chemistry and was successfully applied to certified reference materials and real water samples.

INTRODUCTION

The determination of heavy metals in food and water samples at trace levels is crucial because of their effects on human health and the environment (1). Several techniques commonly used for heavy metal analysis in water include flame atomic absorption spectrometry (FAAS) (2-5), electrothermal atomization atomic absorption spectrometry (ETAAS) (8-13), and inductively coupled plasma-optical emission spectrometry (ICP-OES) (6-7, 14-17). ICP-OES is an efficient technique to determine inorganic elements in environmental and biological samples, and has the ability of multi-element analysis and a high rate analytical efficiency. However, this technique presents reasonable measurability but requires a pre-concentration process for metals determination (18).

Metal ion levels are very low in the samples and detection is quite difficult because of the complex ingredients of the matrix. For that reason, pre-concentration and separation technologies (19-21) are used to extract these metals at proper concentrations. These techniques are liquid-liquid extraction (22, 23), solid phase extraction (24-26), co-precipitation (27-29), electrochemical accumulation (30, 31), ion exchange (32, 33), and cloud point extraction (CPE) (34-38). Cloud point extraction is preferred because it is simple, fast, high yielding, requires less toxic organic solvents and is, therefore, in compliance with the green chemistry principle (39).

Cloud point extraction is based on phase separation in aqueous solution of non-ionic surface activated agents. Phase separation occurs when the cloud point temperature has been reached, and phase separation may be observed not only with a temperature change but also with any material added or a pressure change. Most non-ionic surface-activated agents may form mycelium and separate into two phases: (a) the phase which is below the critical mycelium concentration or at equal concentration and (b) the surface-activated rich phase which pre-concentrates the analyte ions (40, 41). Metal ion complexes are created with the hydrophobic ligand of the surface-active rich phase environment and are separated by the other phase by staying in the mycelium created by the surface-activated material (42).

The internal standard method was used in order to balance non-spectral interferences, decrease the noise and to eliminate the multiple errors in the ICP devices. This method is based on measurement and calculation of the reference element comparative to its signal instead of measuring the emission of the analyte (43, 44).

In this study, pre-concentration and determination of the Cu^{2+}, Cd^{2+}, Pb^{2+}, Co^{2+}, Ni^{2+}, and Zn^{2+} ions are performed by using the indium internal standard and ICP-OES with the cloud point extraction method and an ultrasonic nebulizer. The ultrasonic nebulizer increases the analytical capacity due to the higher vapor efficiency. The aerosol formation is more efficient at making small droplets and removes the solvent, thus giving a 10 times better detection limit (45, 46). The complexing agent 5,7-diiodo-8-hydroxyquinoline was

**Corresponding author.*
E-mail: dundar@sakarya.edu.tr
Tel: +90 264 2956044
Fax: +90 264 2955950

used with Triton® X-114 as the surface-activated agent. The method was applied to the analysis of certified reference material and real water samples.

EXPERIMENTAL

Instrumentation

A model Spectro Arcos ICP-OES (Spectro Arcos, Germany) was used to determine the metal concentrations and was equipped with a CETAC U-5000AT+ ultrasonic nebulizer. The optimum instrumental conditions are listed in Table I. The pH measurements were performed using the Orion 2-Star Plus pH meter (Thermo Scientific, USA) and a NF 400 centrifugation system (Nüve Co., Turkey). A Milli-Q® (18.2 MΩ·cm^{-1}) Integral Water Purification System was used to produce distilled de-ionized ultrapurified water (Millipore Corporation, USA).

Reagents and Standard Solutions

All chemicals used were of analytical grade. The metal solutions were prepared with 1000 mg/L of Cu^{2+}, Cd^{2+}, Pb^{2+}, Co^{2+}, Ni^{2+}, and Zn^{2+} standard solutions (Merck, Germany). Adjustment of the solutions to the proper pH was performed with 0.1 M NaOH and 0.1 M HCl (Merck) solutions, then the proper buffers were added. The hydrophobic complexing agent of 5,7-diiodo-8-hydroxyquinoline was used and 1,1,3,3-tetramethylbuthyl (Triton X-114) as the surface-activated agent with the metal ions. A 5 g amount of Triton X-114 in analytical purity was dissolved in boiling ultrapure water and the volume of the solution completed to 100 mL, resulting in a 5% (w/v) surfactant solution. In order to dilute the surface-active rich phase, ultra-purified 2 mol L^{-1} HNO_3 solution (Merck) was used. For the preparation of the solutions, distilled deionized water (Milli-Q Millipore 18.2 MΩ·cm-1 resistance) was used. An internal standard solution was prepared from 1000 mg/L In (Sigma-Aldrich) stock solution.

TABLE I
ICP-OES and Ultrasonic Nebulizer Operating Conditions

ICP-OES Spectrometer	
Viewing Height	12 mm
Element Wavelength	Cd: 214.438 nm
	Co: 228616 nm
	Cu: 324.754 nm
	Ni: 231.604 nm
	Pb: 220.353 nm
	Zn: 213.856 nm
Replicates	3
RF Power	1450 W
Spray Chamber	Cyclonic
Nebulizer	Modified Cetac ultrasonic nebulizer
Nebulizer flow	0.8 L/min
Plasma Gas Flow	13 L/min
Auxiliary Gas Flow	0.7 L/min
Sample Aspiration Rate	2.0 mL/min
Sample Pump Rate	25 rpm
Ultrasonic Nebulizer Conditions	
Desolvation Temperature	140 °C
Condenser Temperature	5 °C

Sampling

The drinking water and river water samples were obtained in 2015 from the Sakarya river in Adapazari city, Turkey. Polyethylene bottles were used to store the samples which were adjusted to the appropriate pH with HNO_3. Then the samples were filtered with a Millipore nitrocellulose membrane (pore size 0.45 mm) and stored at +4 °C in a refrigerator to prevent microbial activity.

Cloud Point Extraction Procedure

In order to perform cloud point extraction, 10^{-2} mol L^{-1} 5,7-diiodo-8-hydroxyquinoline, buffer, and 5% (w/v) Triton X-114 solutions were added to the various analyte solutions in the range of 10-500 µg L^{-1} concentration and diluted to 50 mL. This solution was placed into a water bath at 55 °C for 20 minutes and centrifuged for 10 minutes at 4000 rpm. It was then soaked in the ice bath for 20 minutes to increase the viscosity of the surface-active rich phase, and the liquid phase of the solution was removed with a micropipette. Following the cooling procedure and because the surface-active rich phase obtained at the bottom of the test tube is viscose, the separation operation can be easily performed. The indium added into the separated surface-active rich phase was diluted with 2 mol L^{-1} HNO_3 solution to 2 mL, and the solution analyzed by USN-ICP-OES.

RESULTS AND DISCUSSION

Effect of pH

Because the pH is one of the basic parameters in complexation

reactions, it is the first variable that has to be examined. Scanning was performed between the pH levels of 2 to 12, and the proper pH value was found between 7–8. It was observed that using this pH, the 5,7-diiodo-8-hydroxyquinoline complexing agent creates the highest and efficient complexes with the Cu^{2+}, Cd^{2+}, Pb^{2+}, Co^{2+}, Ni^{2+}, and Zn^{2+} metal ions. The reason of inefficient recovery on the lowest pH values may be due to the decrease in stability of the metal complexes of 5,7-diiodo-8-hydroxyquinoline. Precipitation of the metals with hydroxides may affect recovery at high pH values. The effect of the pH on the recovery percentages of the metal ions is shown in Figure 1.

Effect of Ligand Concentration

Formation of a hydrophobic and high stability complex with metals of the ligands is significant for the performance of the extraction. 5,7-diiodo-8-hydroxyquinolin forms hydrophobic complexes with the metal ions and pre-concentration is performed by imprisoning these complexes in the mycelium. Because reaction of the metals in the environment of the complexation agent is intended, enough complexation agent is required. Measurements were performed in the concentrations between 0.02 mmol L^{-1} and 0.4 mmol L^{-1}. Recovery values were found to be appropriate at concentrations of 0.08 mmol L^{-1} and above. The possible reason is the increase in complexation efficiency of the excessive ligand molecules and simplification of entrance to the mycelium. The effect of ligand concentration on recovery percentages of the metal ions is shown in Figure 2.

Effect of Triton X-114

Triton X-114 was selected as the surface-activated agent because of high density during phase separation and use of lower mycelium temperature (23-26 °C). The Triton X-114 surface-activated agent was tested between the concentration range of 0.005–0.2% (w/v) which gives the highest recovery rates at 0.04–0.125% (w/v) concentration. Thus, 0.06% (w/v) was chosen as the optimum rate. The effect of the recycling percentage of the metal ions on the surface-activated agent concentration is shown in Figure 3.

Effect of Equilibration Time and Temperature

In order to form stable hydrophobic complexes in cloud point

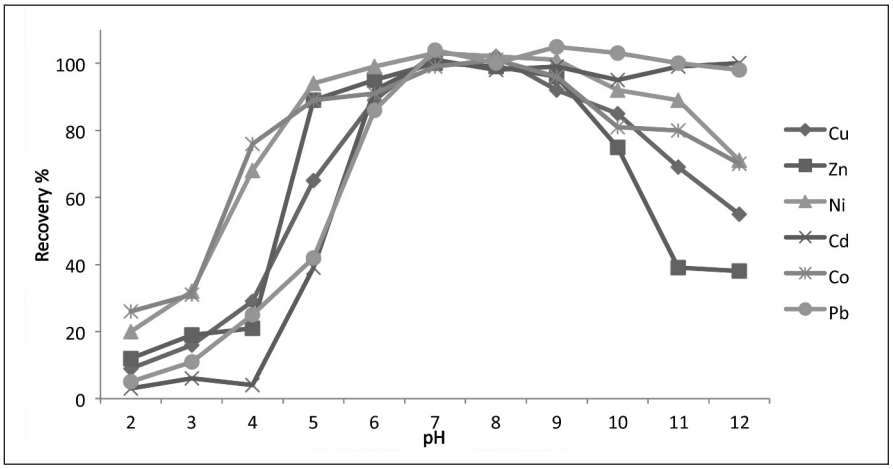

Fig. 1. Effect of pH on the recoveries of the metal ions. Conditions: 50 mL solution, 0.2 mmol L^{-1} 5,7-diiodo-8-hydroxyquinoline, 100 µg L^{-1} metal ions, 0.1% (w/v) Triton X-114.

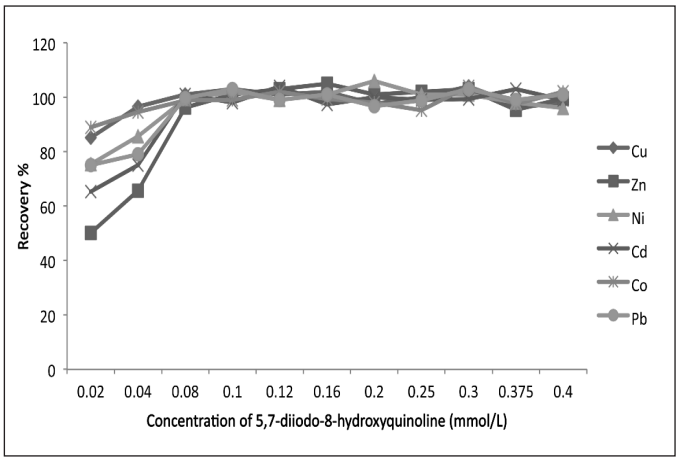

Fig. 2. Effect of complexing agent concentration on the recoveries of the metal ions. Conditions: 50 mL solution, pH 7.0, 100 µg L^{-1} metal ions, 0.05% (w/v) Triton X-114.

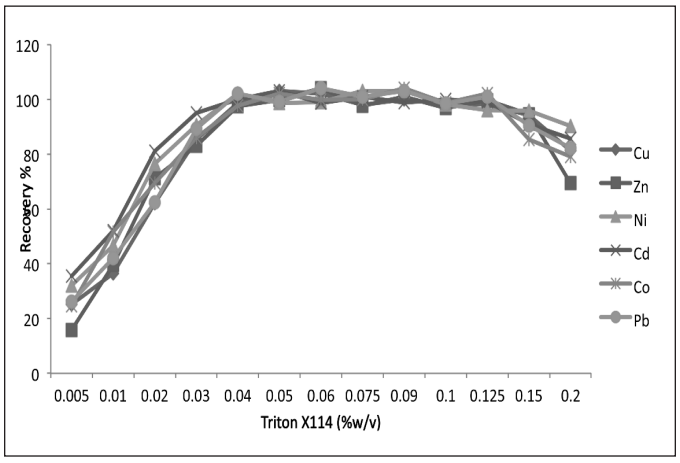

Fig. 3. Effect of Triton X-114 concentration on the recoveries of metal ions. Conditions: 50 mL solution, 0.1 mmol L^{-1} ,5 7-diiodo-8-hydroxyquinoline, pH 7.0, 100 µg L^{-1} metal ions.

extraction and to imprison the hydrophobic structure complexes with the surface-activated agent, the cloud point temperature has to be reached. Complexation efficiency may decrease at low temperatures or remain below the critical concentration of the surface-activated agent. Formations may become unstable at higher temperatures. In this study, it was observed that the recovery value is good for 15 minutes or above and between 45–60 °C. Thus, 20 minutes with 50 °C was the accepted optimum value.

Effect of Interfering Ions

Because of the reasons stated in the previous section, a common ion effect study was performed in order to obtain at least 95% recovery during the enrichment of the metal ions in the presence of various anions and cations. While conducting the experiment, common ion solutions at various concentrations were added to 100 ng mL^{-1} concentrationof the metal ions and cloud point extraction was tested. No undesired interferences were observed up to the specified values as are listed in Table II.

Analytical Performance

After the optimum conditions of the proposed method were obtained, enrichment factor, limit of quantification, limit of detection and precision were calculated as the analytical performance values. The enrichment factor is calculated as the proportion of the slope of the calibration curve obtained by pre-concentration to the slope of the calibration line without preconcentration. The LOD values are calculated using 3 times the 10 independent blank standard deviation divided by the calibration line slope (3σ/m). The LOQ values are calculated using 10 times the standard deviation of the blanks divided by the calibration line slope of (10σ/m). Other measurements and the results are listed in Table III.

TABLE II
Effect of Matrix Ions

Ions	Tolerance Limit
Na^{+}	5000 : 1
K^{+}	5000 : 1
Mg^{2+}	2000 : 1
Ca^{2+}	1000 : 1
Al^{3+}	100 : 1
Ba^{2+}	10 : 1
Fe^{3+}	5 : 1
Cl^{-}	5000 : 1
NO_3^{-}	5000 : 1
F^{-}	5000 : 1
SO_4^{2-}	500 : 1

Analysis of Reference Material and Real Water Samples

Good agreeent of the results of the proposed method was also verified by using the standard reference material (SRM) INCT-TL-1 Tea Leaves (Institute of Nuclear Chemistry and Technology, Poland). For all studies, In was used as the internal standard which was added during the optimization phase resulting in sample measurements at the final value of 100 µg L^{-1}. Excellent recovery of the metals for 500-mL water samles with the cloud point extraction method is demonstrated by using the optimum UN-ICP-OES conditions and the results are listed in Tables IV and V.

CONCLUSION

A method which allows detection of the heavy metals (copper, cobalt, nickel, lead, and cadmium) at trace levels was evaluated. Indium (In) was used as the internal standard, and the internal standard technique is applied successfully in order to prevent the entrance of noise and various interferences. The ultrasonic nebulizer was mounted to the ICP-OES device and similar detection limits of the metals were obtained. The method was also applied to a certified reference material with successful recovery results between 97.4% and 102.7%. Heavy metal ions (Cu^{+2}, Zn^{+2}, Ni^{+2}, Cd^{+2}, Co^{+2}, Pb^{+2}) in water samples

TABLE III
Analytical Performance Parameters of the Proposed Method

Parameters	Cu	Zn	Ni	Cd	Co	Pb
Enrichment Factor	21.04	18.79	21.85	21.73	14.06	13.33
Correlation Coefficient*	0.9984	0.9885	0.9977	0.9987	0.9985	0.9980
RSD (n=10)	3.63	6.28	2.08	2.11	3.45	3.87
LOQ (ng mL^{-1})	0.250	0.99	0.27	0.076	0,1	0,16
LOD (ng mL^{-1})	0.076	0.30	0.081	0.022	0.033	0.049

[a]Correlation coefficient after CPE.

TABLE IV
Analysis of Certified Reference Material for the Determination of Analytes After Application (n=3)

Ions	Certified Values (µg g^{-1})	Values of Present Study (µg g^{-1})	Recovery (%)
Cu	20.400 ± 1.500	20.920±0.460	102.7
Zn	34.700±2.700	33.900±2.960	97.7
Ni	6.120±0.520	5.960±0.960	97.4
Cd	0.030±0.004	0.032±0.003	106.6
Co	0.387±0.042	0.385±0.031	99.5
Pb	1.780±0.240	1.733±0.180	97.4

TABLE V
Recovery of Metals in Water Samples (n=3)

Sample Ions	Added (µg L-1)	Measured (µg L-1)	Recovery (%)
Tap Water			
Cu	0	0.48	
	5	5.45	99.0
	10	10.72	102.4
Zn	0	1.12	
	5	6.27	103.0
	10	11.74	106.0
Ni	0	BDL	
	5	4.9	98.0
	10	10.22	102.0
Cd	0	BDL	
	5	5.05	101.0
	10	9.94	99.0
Co	0	BDL	
	5	4.82	96.0
	10	10.18	102.0
Pb	0	BDL	
	5	5.23	105.0
	10	10.32	103.0
River Water			
Cu	0	1.62	
	5	6.69	101.0
	10	11.91	103.0
Zn	0	3.22	
	5	8.43	104.0
	10	13.9	107.0
Ni	0	0.57	
	5	5.61	101.0
	10	10,23	97.0
Cd	0	BDL	
	5	4.86	97.0
	10	9.77	98.0
Co	0	BDL	
	5	5.31	106.0
	10	9.78	98.0
Pb	0	BDL	
	5	5.19	104.0
	10	10.07	101.0

BDL : Below detection limit.

are enriched by using cloud point extraction and at optimum conditions the limit of detection of the metals were found at 0.076, 0.30, 0,081, 0.022, 0.033, and 0.049 µg L^{-1}, respectively. Also, an enrichment factor between 13.33 and 21.85 was obtained. This study shows a method which can perform metals detection in accordance with the green chemistry concept by eliminating the harmful use of chemicals. In addition, the method is fast, simple, efficient, and low cost for use in the determination of heavy metals at the µg L^{-1} levels.

Received January 17, 2018.

REFERENCES

1. H. Altundag, S. Albayrak, M. S. Dundar, M. Tuzen, and M. Soylak, At. Spectrosc. 34(2), 159 (2015).
2. S. Candir, I. Narin, and M. Soylak, Talanta 77, 289 (2008).
3. V. A. Lemos, J. S. Santos, and P.X.J. Baliza, Braz. Chem. Soc. 17, 30 (2006).
4. H. Altundag, M. S. Dundar, S. Doganci, M. Celik, and M. Tuzen, J. AOAC Int. 96(1), 166 (2013).
5. Z. F. Fan, Microchim. Acta 152 29 (2005).
6. J. H. Wang, E. H. Hassen, and B. Gammelgard, Talanta 55 117 (2001).
7. M. A. M. Silva, V. L. A. Frescura, and A. J. Curtius, Spectrochim. Acta Part B 56(10), 1941 (2001).
8. X. S. Zhu, X. H. Zhu, and B. S. Wang, Microchim. Acta 154 95 (2006).
9. T. A. Maranhao, D. L. G. Borges, M. A. M. L. Veiga, and A. J. Curtius, Spectrochim. Acta Part B 60(5), 667 (2005).
10. H. B. Sang, P. Liang, and D. J. Du, J. Hazard. Mater. 154, 1127 (2008).
11. F. Shemirani, M. Baghdadi, M. Ramezani, and M. R. Jamali, Anal. Chim. Acta 534, 163 (2005).
12. D. L. G. Borges, M. A. M. S. Veiga, V. A. L. Frescura, B. Welz, and A. J. Curtius, J. Anal. At. Spectrom. 18, 501 (2003).
13. F. Shemirani, M. Baghdadi, and M. Ramezani, Talanta 65, 882 (2005).
14. N. Ozcan, and H. Altundag, B. Chem. Soc. Ethiopia 27(2), 205 (2013).
15. Y. J. Li, and B. Hu, J. Hazard. Mater. 174, 534 (2010).
16. H. Altundag, Fresen. Environ. Bull. 24(12a), 4452 (2015).
17. S. Shariati, Y. Yamini, and M. K. Zanjani, J. Hazard. Mater. 156, 5833 (2008).
18. C. R. T. Tarley, S. L. C. Ferreira, and M. A. Z. Arruda, Microchem. J. 77, 163 (2004).
19. M. Ghaedi, F. Ahmadi, and M. Soylak, J. Hazard. Mater. 147, 226 (2007).
20. M. Ghaedi, F. Ahmadi, and A. Shokrollahi, J. Hazard. Mater. 142, 1158 (2007).
21. M. Ghaedi, F. Ahmadi, Z. Tavakoli, M. Montazerozohori, A. Khanmohammadi, and M. Soylak, J. Hazard. Mater. 152, 1248 (2008).
22. T. Wanga, C. Lia, K. Sakanishia, T. Nakazatob, H. Taob, T. Takanohashia, T. Takaradac, and I. Saitoa, Fuel. 84, 1487 (2005).
23. Y. Okamoto, Y. Nomura, H. Nakamura, K. Iwamaru, F. Fujiwara, and T. Kumamaru, Microchem. J. 65, 341 (2000).
24. G. P. C. Rao, S. S. Veni, K. Pratap, Y. K. Rao, and K. Seshaiah, Anal. Lett. 39, 1009 (2006).
25. M. Soylak, and M. Tuzen, J. Hazard. Mater. 137, 1496 (2006).
26. E. Akyuz, M. Imamoglu, and H. Altundag, Atom. Spectrosc. 34(4), 146 (2013).
27. M. Soylak, and N. D. Erdogan, J. Hazard. Mater. 137, 1035 (2006).
28. J. Liu, H. Chen, X. Mao, and X Jin, Int. J. Environ. Anal. Chem. 76, 267 (2000).
29. S. Saracoglu, M. Soylak, D. S. Kacar Peker, L. Elci, W. N. L. dos Santos, V. A. Lemos, and S. L. C. Ferreira, Anal. Chim. Acta 575, 133 (2006).
30. H. Matusiewicz, and M. Lesinski,

Int. J. Environ. Anal. Chem. 82, 207 (2002).

31. J. Komarek, P. Stavinoha, S. Gomiscek, and L. Sommer, Talanta 43, 1321 (1996).
32. Z. T. Jiang, J. C. Yu, and H. Y. Liu, Anal. Sci. 21, 851 (2005).
33. Z. Fang, J. Ruzicka, and E. H. Hansen, Anal. Chim. Acta 164, 23 (1984).
34. L. Tavakoli, Y. Yamini, H. Ebrahimzadeh, A. Nezhadali, S. Shariati, and F. Nourmohammadi, J. Hazard. Mater. 152, 737 (2008).
35. J. L. Manzoori, H. Abdolmohammad-Zadeh, and M. Amjadi, J. Hazard. Mater. 144, 458 (2007).
36. Z. Fan, and F. Bai, At. Spectrosc. 28, 30 (2007).
37. M. Ghaedi, A. Shokrollahi, K. Niknam, E. Niknam, A. Najibi, and M. Soylak, J. Hazard. Mater. 168, 1022 (2009).
38. W. I. Mortada, A. Z. Ali, and M. M. Hassanien, Anal. Meth. 5, 5234 (2013).
39. A. Anastas, and N. Eghbali, Chem. Soc Rev. 39, 301 (2010).
40. M. Ghaedi, A. Shokrollahi, K. Niknam, E. Niknam, S. Derki, and M. Soylak, J. AOAC Int. 92, 907 (2009).
41. H. Filik, T. Cengel, and R. Apak, J. Hazard. Mater. 169, 766 (2009).
42. C. B. Ojeda, and F. S. Rojas, Anal. Bioanal. Chem. 394, 759 (2009).
43. H. Kola, and P. Peramaki, Spectrochim. Acta Part B 59, 231 (2004).
44. G. A. Zachariadis, and D. C. Vogiatzis, Appl. Spectrosc. Rev. 45, 220 (2010).
45. M. A. M. Silva, V. L. A. Frescura, and A. J. Curtius, Spectrochim. Acta Part B 55, 803 (2000).
46. R. I. Botto, J. Anal. Atom. Spectrom. 8, 51 (1993).

Solid Phase Extraction Containing Multi-walled Carbon Nanotubes and Eggshell Membrane as Adsorbent for ICP-OES Determination of Pb(II) and Cd(II) in Various Water and Orange Fruit (Peel and Pulp) Samples

Ali I. Khaleel[a], Ahmed Raoof*[,a], and Mustafa Tuzen*[,b,c]

[a] College of Science, Chemistry Department, Tikrit University, Tikrit, Iraq

[b] Tokat Gaziosmanpasa University, Faculty of Science and the Arts, Chemistry Department, 60250 Tokat, Turkey

[c] King Fahd University of Petroleum and Minerals, Research Institute, Center for Environment and Water, 31261 Dhahran, Saudi Arabia

ABSTRACT

Multi-walled carbon nanotubes (MWCNTs) functionalized with soluble eggshell membrane protein (SEP) bio-polymer were prepared as a novel adsorbent for solid phase extraction and ICP-OES determination of Pb(II) and Cd(II). This material was characterized by FTIR, TG-DTA, DSC, and XRD. Also, a new dithiocarbamate chelating agent derived from barbituric acid was prepared and characterized by FTIR, ^{1}HNMR, and elemental analysis. Various factors influencing the preconcentration of lead and cadmium ions such as pH, sample and eluent flow rates, concentration and type of eluents, sample volume, chelating agent concentration and interfering ions were investigated. The accuracy of the method was confirmed with the standard addition method. The limits of detection (LODs) for this method were found to be 0.10 μg L^{-1} and 0.073 μg L^{-1} for Pb(II) and Cd(II), respectively. The relative standard deviation (RSD) was 1.2% for lead and 1.0% for cadmium, with a preconcentration factor of 25. The optimized method was applied to various water and orange fruit (peel and pulp) samples.

INTRODUCTION

Transition and non-transition elements with a density of at least five times that of water and a high atomic weight, such as cadmium (Cd) and lead (Pb), are considered heavy metals which are also very toxic to the human body and cause environmental pollutants (1). Therefore, the accurate determination of heavy metals at trace levels in foods and water is very important. Solid phase extraction (SPE) techniques have been used to overcome the problems of determining elements at low levels because it increases the sensitivity and selectivity of the techniques such as ICP-OES, AAS, etc. For SPE, the use of nano-sized sorbents has been proposed to extract the elements onto large surface areas (2-4). In addition, carbon nano-sized materials, such as carbon nanotubes (CNTs), graphene oxide, etc., have been used in SPE but these materials are very expensive (5-9).

For this reason, a novel biopolymer has been investigated, such as eggshell membrane, either alone or mixed with nano-materials (10-12). Some researchers used chelating agents to increase the extraction of the metal ions after formation of a macro-compound (as complex with the chelating agent) (13, 14).

*Corresponding author.
E-mail: ahmedbayatli89@gmail.com,
E-mail: mustafa.tuzen@gop.edu.tr
Tel: +90 356 2521616
Fax: +90 356 2521585

In the present research, multi-walled carbon nanotubes (MWCNTs) were oxidized in order to add many functional groups (carboxyl groups) onto the surfaces which then easily react with the protein derived from the soluble eggshell membrane protein (SEP). Barbituric acid (Bis-sodium barbituric acid dithiocarbamate) (BADTC) was used as the chelating agent to enhance the extraction of cadmium and lead. An optimized method was applied to five water and 10 orange fruit (five peel and five pulp) samples for the ICP-OES determination of cadmium and lead.

EXPERIMENTAL

Instrumentation

The infra-red spectra were recorded with an FTIR-8400S spectrophotometer within the range of 400-4000 cm^{-1}, and the X-ray diffraction measurements by using an XR – 6000 device with a nickel-copper filter for X-ray radiation (Cu Kα, λ = 1.5406 Å) (Shimadzu, Japan). The lead and cadmium ions were determined using the iCAP™ 7000 Series ICP-OES (Thermo Scientific, UK). Thermogravimetric analysis (TG/DTA) was performed using the a PYRIS Diamond TG/DTA apparatus (PerkinElmer, Inc., Shelton, CT, USA), and for differential scanning calorimetry the DSC 131 instrument (Setaram Instrumentation, France) was used.

Reagents and Solutions

The Pb(II) and Cd(II) standard stock solutions (1000 mg/L) were obtained from Sigma-Aldrich Company, USA. Deionized water was used for solution preparation using the Milli-Q® system, 18.2 MΩ·cm^{-1} conductivity (Millipore Corporation, USA). Buffer solutions of

KH_2PO_4-NaOH (pH 3–8), NH_4Cl-NH_3 (pH 9–11), and 0.02 mol L^{-1} HNO_3 were used for maintaining the pH at less than 3 (Alfa-Aesar, USA). Sulfuric acid, thioglycolic acid, and nitric acid were purchased from (HI-MEDIA, USA). The multi-walled carbon nanotubes (MWCNTs, O.D. × L 7-15 nm × 0.5-10 µm) were purchased from Sigma-Aldrich, USA.

Bis-sodium Barbituric Acid Dithiocarbamate (BADTC)

To a solution of barbituric acid (0.8 g, 6 mmol) in 20 mL of DMSO, CS_2 (0.48 g, 6 mmol) was added in the presence of NaOH (0.25 g, 6 mmol). The reaction was maintained at 0–3 °C using a water-ice bath. This mixture was continuously stirred for 3 hours. The obtained pink precipitate was then filtered and washed with benzene. The product was dried in a vacuum oven at 100 °C, m.p >320. The analytical calculation for $C_6H_2N_2Na_2O_3S_4$ (%): C, 22.22; H, 0.62; N, 8.64; was found at C, 22.32; H, 0.66; N, 8.75, yield 93%. FTIR (KBr): 2922w, 2819w, 1685vs, 1630vs, 1500s, 1412m, 1356m, 911m, 1097m cm^{-1}, 1H-NMR(∂^6-dmso): (∂, 3.25 ppm, 2H).

Synthesis of Soluble Eggshell Membrane Protein (SEP)

Eggshells (250 g) were washed several times with deionized water to remove the albumin. Then they were immersed in 500 mL of 2% acetic acid at 25 °C for 1 hour in order to release the eggshell membrane (ESM). This membrane was washed with deionized water to remove excess acetic acid, dried at 80 °C for 6 hours, and ground. Then, 10 g of ESM powder was immersed in 150 mL of 1.2 N of thioglycolic acid and 10% acetic acid aqueous solution, sonicated for 1 hour at 25 °C to form a suspension, and refluxed for approximately 30 hours until the ESM completely dissolved (11, 15, 16).

Preparation of MWCNTs-SEP Nano-sorbent

The MWCNTs were first oxidized by refluxing 1 g of MWCNTs in 3:1 H_2SO_4: HNO_3 at 75 °C for 5 hours (13, 14). The mixture was centrifuged at 8000 rpm and the supernatant dried, then the SEP solution was added to the filtered oxidized MWCNTs powder, sonicated for 2 hours, and refluxed for 8 hours at 80 °C. The greyish powder was filtered, washed with water and ethanol, then dried for 24 hours at 80 °C.

Preparation of Column

An amount of 0.3 g of the prepared nano-material (MWCNTs-SEP) was packed into a glass column (10x100 mm) and both the upper and lower ends were closed with glass wool. The column was connected to a pump with tubing which formed the preconcentration system. A 2 mol L^{-1} amount of HNO_3 aqueous solution and 10 mL of deionized water were passed through the column to clean it, then it was conditioned to the required pH with buffer solution.

Preconcentration Procedure

Amounts of 40-50 mL model solutions containing Pb(II) and Cd(II) ions were buffered to pH 7 with borate buffer solution, Then $3.2.10^{-3}$ mol L^{-1} BADTC ligand solution was added for metal-chelate formation and passed through the MWCNTs-SEP column at the 5 mL/min flow rate. Control of the flow rate of the sample into the extraction column was performed by gravity. The adsorbed analyte ions were eluted using 2 mol L^{-1} HNO_3 and the eluent solution containing the Pb(II) and Cd(II) ions was analyzed by ICP-OES.

Application to Orange (Peel, Pulp) and Water Samples

The nano-sorbent-containing column was utilized for the preconcentration and determination of lead and cadmium in 10 orange (peel or pulp) and five water samples (well water, wastewater, tap water, drinking water, and river water) obtained from Kirkuk city, Iraq. The whole orange was washed with deionized water. The orange peel and pulp were separated, and dried in an oven at 100 °C for 48 hours, then crushed, and 1 g of each orange fruit part (peel or pulp) was acidified with HNO_3 (65%) and heated at 120 °C under constant stirring for 4 hours. Then the residue was placed into an automatic shaker for 1 hour, filtered, and diluted up to 50 mL of 1% HNO_3 aqueous solution.

Different water samples were filtered in Fisherbrand™ Grade 601 filter paper. Then 100 mL of these solutions was used for ICP-OES determination of total Pb(II) and Cd(II) concentration using the optimum conditions described earlier.

Characterization of Prepared Materials

FTIR Analysis

The FTIR spectrum of MWCNT-COOH is shown in the bands at 3749 cm^{-1}, 3477 cm^{-1}, 1754 cm^{-1}, 1649 cm^{-1}, and 1510 cm^{-1}. These bands represent the free hydroxyl group, the OH stretching vibration of the carboxylic group, stretching vibration of C=O in the carboxyl group, as well as the bending vibrations of the water and carboxylate anion, respectively (17-20).

The FTIR spectrum of SEP is shown with 9 main bands (3292, 3072, 1658, 1546, and 1396 cm^{-1}). These bands can be attributed to the stretching vibration of NH, C-H of the aromatic ring, amide (I), amide (II), and C-N, respectively. The other peaks at 2962 and 2931 cm^{-1} are due to the stretching vibration of aliphatic C-H, while the two bands at 2634 and 2546 cm^{-1} are attributed to the thiol groups that

formed after the dissolving process with thioglycolic acid (16, 21).

The FTIR spectrum of MWCNTs-SEP shows all characteristic bands of the MWCNTs and SEP, but shifting of the carbonyl group of MWCNTs-COOH from 1745 cm^{-1} towards the lower wavenumber of 1713 cm^{-1} of MWCNTs-SEP. In addition, the disappearance of the NH band at 3292 cm^{-1} of SEP and the OH band at 3477 cm^{-1} of MWCNTs results in the reaction of MWCNTs with SEP from the carboxyl of MWCNT and the amine of the amide group in SEP.

TGA/DTA and DSC Analyses

TG was used to determine the amount of SEP reacting with the MWCNTs by comparing the mass loss found between the MWCNTs and the MWCNTs-SEP during heating (see Figure 1). After functionalization of the SEP, mass loss started at 80 ºC, which can be attributed to 3.5% of water evaporation. Continuing heating from 120 to 440 ºC resulted in a 74.0% decomposition of the SEP. The degree of gradual mass loss of the MWCNTs-SEP was expected to be around 74.0%. While the MWCNTs show a single-step decomposition at ~637 ºC and totally oxidize around 700 ºC (22), therefore the MWCNTs quantity did not exceed 22.5%.

The DSC thermogram for the MWCNTs-SEP showed three main peaks: 168.6 ºC, 218.7 ºC, and 433.0 ºC (Figure 2). The peak observed at 218.7 ºC was much larger than at the other temperatures. This broad peak due to the heat flow required denaturing of the amino acids in the SEP.

XRD Analyses

The eggshell membrane protein is amorphous material and, therefore, no peak could be detected by XRD analysis. The peaks that appeared are attributed to calcium impurities in the egg shell.

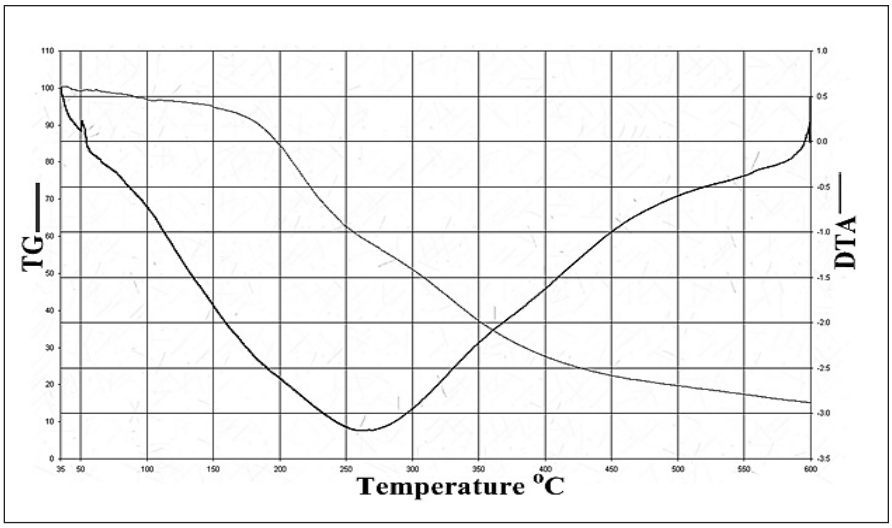

Fig. 1. TG/DTA thermogram of MWCNTs-SEP.

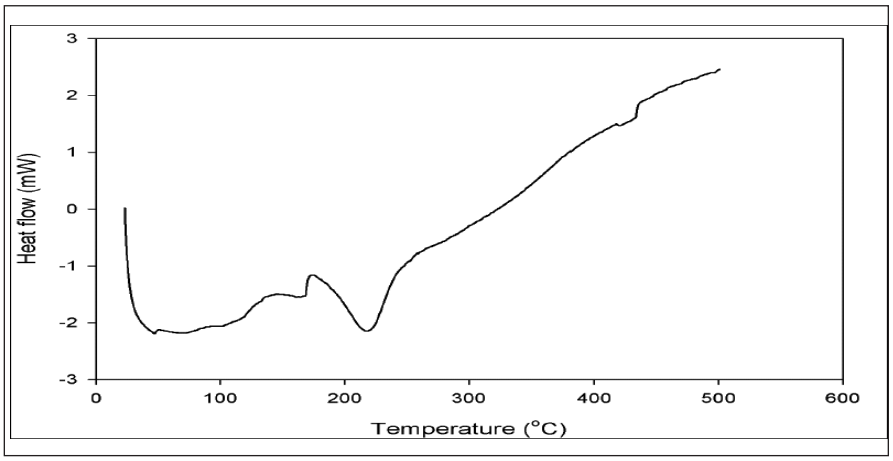

Fig. 2. DSC thermogram of MWCNTs-SEP.

MWCNT-COOH shows two characteristic broad peaks at 2θ = 26.10 and 2θ = 430 (23). After reaction with the SEP, the first peak shifted towards lower values at 2θ = 25.890, while the second peak shifted to higher values at 2θ = 44.250 (Figure 3). This indicates that MWCNT-COOH was successfully grafted onto the SEP. The XRD pattern of the MWCNTs-SEP was used to calculate the crystalline size estimated by the Debye–Scherer equation:

$$d = K \lambda/\beta \cos \theta$$

where λ is the X-ray wavelength (0.1540 nm), K is a constant related to the crystallite shape mostly equal to 0.9, β is the peak width of the diffraction peak shape at half the maximum height FWHM resulting from the small crystallite size in the radians.

From the Debye–Scherer equation for the four characteristic peaks of MWCNTs-SEP listed in Table I, the average crystalline size was found to be 26.72 nm. This increase in the size of the MWCNTs from approximately 10 to 26.72 nm proves that MWCNTs have successfully grafted with SEP.

RESULTS AND DISCUSSION

Effect of pH

The quantitative recoveries of Pb(II) and Cd(II) in the SPE process depend on many conditions, the most important being the pH (24, 25). Therefore, the effect of pH ranging from 2 to 11 on the SPE of Pb(II) and Cd(II) using the new sorbent was examined (see Figure 4). Quantitative recovery for Pb(II) was 98% and 96% for Cd(II). Thus, for all subsequent experiments, pH 7 was carried out with borate buffer solution.

Effect of Flow Rates

Sample and eluent flow rates are very important for the quantitative recovery of analytes and were examined in the range of 0.5–5.0 mL/min from the MWCNTs-SEP column. The optimal sample and eluent flow rates for both Cd(II) and Pb(II) were found to be 5 mL/min. The quantitative recoveries based on the eluent flow rates were 96% for Pb(II) and 95% for Cd(II), but the recoveries with the sample flow rates were 97% for Pb(II) and 98% for Cd(II).

Effect of Different Eluents and Their Concentrations

Desorption of Pb(II) and Cd(II) from the MWCNTs-SEP column was studied using three different types of eluent solutions: HNO_3, HCl, and HNO_3 in acetone. The highest recovery of the analyte ions was found with 2 mol L^{-1} HNO_3 for Cd(II) and Pb(II). The volume of the eluent solution is also very important for obtaining a high preconcentration factor. For this study, the minimum eluent concentration was found with 4 mL 2 mol L^{-1} HNO_3 for both Cd(II) and Pb(II)

Effect of Sample Volume

Since sample volume affects the recovery of Pb(II) and Cd(II), this parameter was examined in the range of 5-100 mL with flow rates at 5 mL/min. The optimal sample volume was recorded to be 100 mL for both Cd(II) and Pb(II) and was selected for further work. The recorded quantitative recoveries were 95% for Pb(II) and 96% for Cd(II). The preconcentration factor, defined as the ratio of the highest sample volume (100 mL) to minimum eluent volume (4 mL 2 mol L^{-1} HNO_3) was calculated as 25.

Effect of Chelating Agent Concentration

BADTC was used as the chelating agent for optimization of the SPE process of Pb(II) and Cd(II).

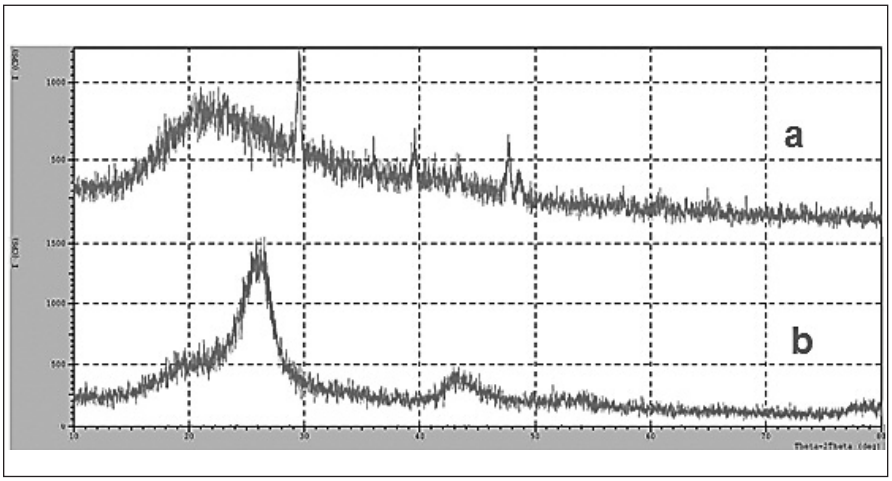

Fig. 3. XRD of (a) ESM and (b) MWCNTs-SEP in the 2θ range of 10-80 degrees.

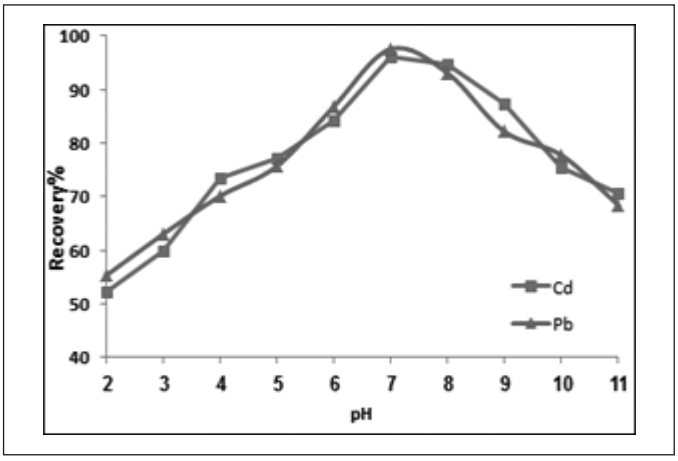

Fig. 4. Effect of pH on the recovery of analytes (N=3).

TABLE I
XRD Debye-Scherrer Equation for the Four Characteristic Peaks of MWCNTs-SEP

Peak Position 2θ (deg.)	FWHM (deg.)	Dp (nm)
25.8994	2.72	3.13
19.3149	0.86	9.79
44.2512	1.08	8.30
28.7550	0.10	85.72

This chelating agent plays a main role in the extraction and recovery of the studied analyte ions and is due to the presence of many functional groups which are able to coordinate with the lead and cadmium ions. BADTC (0–0.008 mol L^{-1}) was added to a model solution containing Pb(II) and Cd(II) for metal-chelate formation, then passed through the column. The results show that quantitative recoveries were obtained with $3.2*10^{-3}$ mol L^{-1} BADTC for both Pb(II) and Cd(II).

Effect of Interfering Ions

This parameter was examined by adding different concentrations of interfering ions because it may decrease or increase the recovery of Pb(II) or Cd(II). The results show that the maximum tolerance of the studied cations and anions cause a relative error of not more than 5% (see Table II). The tolerans limits of the matrix ions were very high, which shows that the present method can be applied to high saline and complex matrix media.

Analytical Figures of Merit

The limit of detection (LOD) of the present MWCNTs-SEP column for the SPE process of Pb(II) and Cd(II) was performed under the optimal conditions after application of the procedure to a blank solution. Based on three times the standard deviation of 10 runs of the reagent blank solution, the LODs were found to be 0.10 μg L^{-1} and 0.073 μg L^{-1} for Pb(II) and Cd(II), respectively. The relative standard deviation (RSD %) of this study was 1.2% for Pb(II) and 1.0% for Cd(II), and the preconcentration factor was 25. The accuracy of the present SPE method was confirmed with the standard addition method.

Table II
Effect of Interfering Ions (N=3)

Ion	Conc. (mg L^{-1})	Recovery% Cd(II)	Pb(II)
Na^+	10,000	96±1	97±1
K^+	13,000	96±2	98±3
Cl^-	20,000	97±1	98±1
Mg^{2+}	5000	96±4	96±1
Cu^{2+}	20	98±3	68±3
Ni^{2+}	25	98±3	96±2
Co^{2+}	20	97±2	96±3
CO_3^{2-}	4500	98±1	98±1
Fe^{3+}	40	96±4	98±2
NO_3^-	4500	95±2	98±3
SO_4^{2-}	4500	98±3	97±1
PO_4^{3-}	4500	96±1	96±3
Zn^{2+}	20	98±3	95±2
Ca^{2+}	5000	99±4	96±3

Application to Various Water and Orange Fruit (Peel and Pulp) Samples

The present MWCNTs-SEP column/SPE method was applied to various water samples by using the standard addition method (see Table III). Quantitative recovery values were found in the samples for Pb(II) and Cd(II). The MWCNTs-SEP column using the SPE method was also applied to 10 orange fruits (five peel and five pulp) samples. The results in Table IV show that the MWCNTs-SEP sorbent can be used as an effective solid phase extraction (SPE) method.

CONCLUSION

In this work, a new nano-sorbent was prepared from soluble eggshell membrane (ESM) on multiwalled carbon nanotubes (MWCNTs). This nano-sorbent is economical and eco-friendly and was used to extract and preconcentrate Pb(II) and Cd(II) for ICP-OES determination in orange fruit (peel or pulp) samples and five water samples. The advantages of this method include simplicity, sensitivity, and require no organic solvents. In addition, by using the newly prepared chelating agent (BADTC), the extraction process was enhanced because of the seven active sites

TABLE III
Determinations of Pb(II) and Cd(II) in Water Samples After Application of Present Method (N=3)*

Sample	Pb(II) Added (μg L^{-1})	Found (μg L^{-1})	Recovery (%)	Cd(II) Added (μg L^{-1})	Found (μg L^{-1})	Recovery (%)
Well Water	–	BDL		–	BDL	
	10	9.9±2.3	99	1.0	0.98±0.21	98
	50	49.5±1.4	99	3.0	2.98±0.21	99
Drinking		—	BDL		—	BDL
Water	20	10.1±1.1	101	1.0	0.98±0.06	98
	20	19.6±2.1	98	3.0	3.04±0.20	101
River Water	—	BDL		—	BDL	
	10	9.7±3.2	97	5.0	4.99±0.01	99
	20	19.8±2.3	99	10	10.0±0.1	100
Tap Water	—	BDL		—	BDL	
	10	10.1±1.3	101	5.0	4.93±1.01	98
	20	19.5±2.0	97	10	9.72±0.24	97
Wastewater	—	BDL		—	BDL	
	10	10.2±3.0	102	5.0	5.01±2.31	100
	20	19.7±2.3	98	10	10.1±0.40	101

*N=3, mean ± S.D, BDL: below the detection limit.

TABLE IV
Determinations of Pb(II) and Cd(II) in Orange Fruit (Peel and Pulp) Samples

Sample	Pb(II) Added (μg L^{-1})	Pb(II) Found (μg L^{-1})	Pb(II) Recovery (%)	Cd(II) Added (μg L^{-1})	Cd(II) Found (μg L^{-1})	Cd(II) Recovery (%)
AA	—	BDL		—	BDL	
	1.0	0.98±0.23	98	0.5	0.50±1.13	97
	2.0	1.95±0.31	07	1.0	1.01±1.01	101
aa	—	BDL			—	BDL
	1.0	0.99±0.11	99	0.5	0.48±0.31	96
	2.0	2.03±0.22	101	1.0	0.98±0.21	98
BB	—	BDL			—	BDL
	1.0	0.98±1.3	98	0.5	0.51±2.21	100
	2.0	1.98±2.03	99	1.0	1.00±0.41	100
bb	—	BDL			—	BDL
	1.0	0.96±2.2	96	0.5	0.48±0.21	96
	2.0	1.97±0.3	98	1.0	0.97±0.04	97
CC	—	BDL		—	BDL	
	1.0	0.99±0.41	99	0.5	0.50±1.01	100
	2.0	1.99±1.03	99	1.0	0.98±0.11	98
cc	—	BDL		—	BDL	
	1.0	0.96±1.1	96	0.5	0.49±0.05	98
	2.0	1.98±0.02	99	1.0	1.02±0.21	102
DD	—	BDL		—	BDL	
	1.0	1.01±2.03	102	0.5	0.48±0.04	96
	2.0	2.06±0.15	103	1.0	0.99±0.12	99
dd	—	BDL		—	BDL	
	1.0	1.01±1.03	101	0.5	0.50±2.3	100
	2.0	1.99±0.43	99	1.0	0.99±1.3	99
EE	—	BDL		—	BDL	
	1.0	0.97±2.02	97	0.5	0.48±0.41	96
	2.0	1.99±0.21	99	1.0	0.96±2.31	96
ee	—	BDL		—	BDL	
	1.0	1.00±2.03	100	0.5	0.50±0.15	100
	2.0	1.98±1.21	99	1.0	0.99±2.04	99

*N=3, Mean±SD, BDL: below the detection limit.
AA, BB, CC, DD, EE = Peel
aa, bb, cc, dd, ee = Pulp

available for coordination with the metal ions. The results show that MWCNTs–SEP is a very promising sorbent material for the determination of Pb(II) and Cd(II) in the presence of one of the dithiocarbamate ligands (BADTC). Table V provides a comparison of the present method with literature values and shows that the LOD and RSD values of the present method are lower.

ACKNOWLEDGMENT

The authors are grateful for the support provided by Tikrit University. Dr. Mustafa Tuzen also gives thanks to Gaziosmanpasa University and King Fahd University of the Petroleum and Minerals Research Institute, Center for Environment and Water, for their support.

Received February 1, 2018.

REFERENCES

1. M. Tuzen, E. Sesli and M. Soylak, Food Control. 18, 7 (2007).
2. N. Bilandzic, M. Dokic and M. Sedak, Food Chem. 124, 3 (2011).
3. E.M. Thurman and M.S. Mills, Solid phase extraction: Principles and practice J.D. Winefordner (Ed.), Chemical Analysis, 147. John Wiley and Sons Inc., N.Y., USA (1998)
4. Ö. Yalçınkaya, O. M. Kalfa, A. R. Türker, Turk. J. Chem. 34, 207 (2010).
5. M. Rahimi amd E. Noroozian, Talanta. 123, 5 (2014).
6. Z.A. Alothman, Y.E. Unsal, M. Habila, M. Tuzen and M. Soylak, Desalin Water Treat. 53, 13 (2015).
7. A.S. Amin and A.A. Gouda, Food Chem. 132, 1 (2012).
8. A.A. Gouda, Int. J. Environ. Anal. Chem. 94, 1210 (2014).
9. D. Mendil, M. Karatas and M. Tuzen, Food Chem. 177, 320 (2015).
10. M. Wang, G. Meng, Q. Huang, H. Tang, Z. Li and Z. Zhang, Sci. China Mater. 58, 198 (2015).

TABLE V
Comparative Data from Some Recent Studies
Using MWCNTs as Solid Phase Extractor

System	Technique	RSD(%) Pb	RSD(%) Cd	LOD (μg L^{-1}) Pb	LOD (μg L^{-1}) Cd	Matrix	Ref.
GO-MCNTs-DETA	ICP-OES	3.0	—	0.24	—	Wastewater	26
MWCNTs/APDC	FAAS	—	>5	0.45	0.6	Food and Environmental	27
MWCNTs	ICP-AES	1.9	1.63	2.1	0.3	Skin	28
MWCNTs-BTAO	FAAS	—	5.0	2.6	0.7	Various Ffoods and Water	14
MWCNTs-Fe_3O_4	ICP-AES	1.23	0.92	0.6	0.3	Water, Milk, Indian Rice, and Red Tea	29
MWCNTs-Tartrazine	FAAS	—	—	6.6	0.8	Food and Natural Water	31
[NMIIM]Br-CSs	FAAS	3.2	—	1.76	—	Waste and Sseawater, Spice, and Street Dust	31
MWCNTs-SEP	ICP- OES	1.2	1.0	0.10	0.073	Water and Oranges	This study

*GO: Graphene oxide; DETA: diethylenetriamine; APDC: Ammonium pyrrolidine dithiocarbamate;
[NMIIM]Br-CSs: 1,8-naphthalene monoimide bearing imidazolium salt ([NMIIM]Br) and IL(ion liquid) coated carbon nano spheres.

11. S. Wang, M. Wei, and Y. Huang, J. Agric. Food Chem. 61, 21 (2013).
13. S. Park, J. An, J.R. Potts, A. Velamakanni, S. Murali and R.S. Ruoff, Carbon. 49, 9 (2011).
12. M. Baláž, Acta Biomater. 10, 9 (2014).
14. A. Gouda and S. AlGhannam, Food Chem. 202, 409 (2016).
15. Y. Zhang, W. Wang, L. Li, Y. Huang and J. Cao, Talanta 80, 5 (2010).
16. F. Yi, Z.X. Guo, L.X. Zhang, J. Yu and Q. Li, Biomaterials 25, 19 (2004).
17. F. A. Abuilaiwi, T. Laoui, M. Al-Harthi and M. A. Atieh, Arab. J. Sci. Eng. 35, 1 (2010).
18. K. Balasubramanian and M. Burghard, Small, 1, 198 (2005).
19. S.K. Mishra, S.N. Tripathi, V. Choudhary and B.D. Gupta, Plasmonics 10, 5 (2015).
20. V.K. Gupta, O. Moradi, I. Tyagi, S. Agarwal, H. Sadegh, R. Shahryari-Ghoshekandi, A.S. Makhlouf, M. Goodarzi and A. Garshasbi, Crit. Rev. Environ. Sci. Technol. 46, 2 (2016).
21. Z. Yu-Hong and C. Yu-Jie, Biotech. 8, 2 (2009).
22. S.P. Lonkar, O.S. Kushwaha, A. Leuteritz, G. Heinrich and R.P. Singh, RSC Adv. 2, 32 (2012).
23. B. Yuan, C. Bao, L. Song, N. Hong, K.M. Liew, and Y. Hu, Chem. Eng. Sci. 237, 3 (2014).
24. Z.A. ALOthman, M. Habila, E. Yilmaz and M. Soylak, Michrochim. Acta 177, 3 (2012).
25. M. Ghaedi, M. Montazerozohori, N. Rahimi and M.N. Biysreh, Ind. Eng. Chem. Res. 19, 5 (2013).
26. X. Zhu, Y. Cui, X. Chang and H. Wang, Talanta.146, 1 (2015).
27. M. Tuzen, K.O. Saygi and M. Soylak, J. Hazard. Mater.152, 2 (2008).
28. A.A. Ayoub, A.A. Mohammad, Z.A. AlOthman and O. Kamal, Int. J. Environ. Res. Public Health 10, 1 (2013).
29. S. Azimi and Z. Es'haghi, Bull. Environ. Contam. Toxicol. 98, 6 (2017).
30. M. Soylak and Z. Topalak, J. Ind. Eng. Chem. 20, 2 (2014).
31. S. Tokalioglu, E. Yavuz, H. Şahan, S.G. Çolak, K. Ocakoglu, M. Kaçer and S. Patat, Talanta 159, 2 (2016).

Response Surface Modeling for Pb(II) Removal From Alcoholic Beverages Using Natural Clay: Process Optimization With Box–Behnken Experimental Design and Determination by Electrothermal AAS

Olcay Kaplan Ince[a], Muharrem Ince[b,*], and Ali Onal[a]

[a] Munzur University, Faculty of Engineering, Department of Food Engineering, 62000 Tunceli, Turkey

[b] Munzur University, Faculty of Engineering, Department of Chemical Engineering, 62000 Tunceli, Turkey

ABSTRACT

A three-level four-factor Box–Behnken experimental design (BBD) combined with response surface modeling (RSM) was used for the optimization and modeling of Pb(II) adsorption from alcoholic beverages onto natural clay. The BBD method was chosen as the statistical prediction method to reduce the experimental numbers which saves time and chemicals and reduce analysis cost. Various independent process variables including solution pH (X_1: 3.0–7.0), contact time (X_2: 2–60 min), adsorbent dosage (X_3: 0.01-0.1 g), and agitation speed (X_4: 50–150 rpm) were optimized. The optimal conditions used for Pb(II) removal were pH of 5.3, contact time 38.9 minutes, 0.071 g adsorbent dosage, and 98.7 rpm agitation speed, resulting in a maximum removal efficiency of 120 mg g^{-1}. Pb was determined by electrothermal AAS.

The significance of the independent variables and their interactions were tested by means of the analysis of variance (ANOVA) and are based on the ANOVA statistical value. The adsorption of Pb(II) onto clay was found to be highly significant with very low probability (p) values (<0.001). These results were justified by the relatively high correlation coefficients (R^2 = 0.9965, R^2 adj = 0.9930, and R^2 Pred= 0.9819) of the statistical prediction. FTIR analysis confirmed major participation of amide, amines, ketones, including the primary alcohol groups, during Pb(II) biosorption. Clay was characterized by Fourier transform infrared spectroscopy (FTIR) and scanning electron microscope (SEM), coupled with energy dispersive X-Ray (EDX). The proposed adsorption process efficiently removes Pb(II) present in various aqueous media and can be used for industrial wastewater or drinks.

INTRODUCTION

The heavy metals Pb, Hg, Cd, Ni, Cr, and Cu persist in nature, bioaccumulate, and are considered toxic and hazardous to humans and other living organisms. In addition, due to rapid technological developments and the use of toxic metals in industry, environmental pollution has become a serious problem for the ecosystem (1-5). Lead is not essential for mammals, and about 800 mg creates toxicity in humans (6-10). Various industries contribute to lead contamination such as electroplating, metal surface finishing, metallurgical, tannery, chemical catalysis, mining, and the manufacture of electrical goods. Bioaccumulation causes severe damage to the kidneys, the nervous and reproductive systems, including the liver and the brain resulting in reduced mental function and damage to blood composition. The U.S. Environmental Protection Agency (USEPA) mandates the maximum contaminant level for lead as 0.015 mg L^{-1}, while the maximum contaminant level goal is zero. In addition, the World Health Organization (WHO) has set a provisional limit of 0.05 mg L^{-1} for Pb (11-15).

Removal of heavy metals, including Ni, Cd and Pb, from various matrices is necessary as these metals directly enter the human food chains, therefore presenting a high health risk to consumers. Recently, this problem has received considerable attention (16).

To remove the metal ions from aqueous solutions, a number of technologies have been developed and include membrane filtration systems, electrochemical technologies, evaporation, coagulation–flocculation, ion-exchange, membrane filtration, reverse osmosis, and adsorption. But all of these techniques have disadvantages and limitations in application. Moreover, some have high operating costs and produce sludges with high concentrations of Pb and other chemical substances. The desorption techniques are widely used as an alternative method for removing dissolved metal ions from liquid media because of simplicity, selectivity, and effectiveness for low metal concentrations (8-10, 17-19). In light of this information, the number of adsorption studies has grown significantly leading to research on the development and optimization of adsorbents, including metallic oxides, clay, biosorbents, zeolites, ion exchange resins, and various polymeric adsorbents, for Pb removal (19-23).

To minimize processing costs, the investigations have focused on

*Corresponding author.
E-mail: muharremince@munzur.edu.tr
Tel: +90 428 213 17 94/2404
Fax: +90 428 213 16 24

the use of ecofriendly and inexpensive adsorbents, as well as using statistical methods, such as the Box-Behnken Design (BBD) with the response surface methodology (RSM) (24-26). BBD is the most commonly used combination design of the RSM model (27, 28) and has been adopted as an experimental design model to study the interactions of combinations of parameters such as solution pH, stirring time, and temperature (29, 30). Its greatest advantage is a reduction in the number of experiments required to interpret multiple parameters and their interactions. The RSM optimization process contains three steps: (a) appropriate experimental design selection, (b) estimation of all of the coefficients of the model using ANOVA, and (c) model validation based on prediction and experimental runs of the process response validation of the final model (31).

The present study is first to report Pb(II) determination in alcoholic beverages using natural locally available clay (Malatya, Turkey) for batch experiments. The RSM method in combination with the BBD was selected to determine and optimize the effects of the process conditions on the response surface analysis of the Pb(II) amount adsorbed on clay. The experimental conditions studied include solution pH, contact time, adsorbent dose, and agitation speed, along with their interactions in Pb(II) adsorption on clay.

EXPERIMENTAL

Instrumentation

A study involving thermal programs for the determination of Pb(II) in several beer and homemade wines by electrothermal atomic absorption (ETAAS) using the AAnalyst™ 800 (PerkinElmer, Inc., Shelton, CT, USA) is presented. The instrumental operating conditions are given in Table I. Because of practicability, sensitivity, precision, and accuracy, ETAAS allows a higher throughput and can be a useful alternative when compared to FAAS, which inevitably requires either a sample pre-concentration or use of the standard additions method.

Chemicals

Lead, sodium hydroxide, hydrochloric acid, and nitric acid were obtained from Merck (Darmstadt, Germany). All chemicals used were of analytical reagent grade.

Preparation of Standard Solutions

A stock solution of 1000 mg L^{-1} Pb(II) was prepared by dissolving an accurate quantity of $Pb(NO_3)_2$ in distilled water. Other concentrations varying from 10 µg L^{-1} to 400 mg L^{-1} were prepared from the stock solutions by dilution.

Box–Behnken Design and Optimization Procedure

A 3-level (low, medium, and high: coded as −1, 0, and +1) 4-factor BBD, combined with RSM, was used to determine the maximum Pb(II) biosorption on clay. The four critical parameters affecting Pb(II) adsorption, namely pH (X_1), contact time (X_2), adsorbent dosage (X_3), and agitation speed (X_4) were selected as independent variables, and removal of biosorption (Y) was considered as the dependent variable (response). Table II lists the independent experimental variables and their levels for adsorption of Pb(II). The experimental results were analyzed using the Design Expert software program (Design Expert, Version 10, Stat-Ease, USA) and the regression model was proposed. Table II also lists the different parameters such as variable conditions, run order, experimental values, and predicted values. The final equation obtained from RSM in terms of actual factors was as follows:

$$Y\ (\mu g\ Pb / mg\ clay) = -549.03 - 169.93X_1 + 261.160.98X_2 + 3809.16X_3 + 1.42X_4 + 0.21X_1X_2 - 64.50\ X_1X_3 - 0.06X_1X_4 + 8.07\ X_2X_3 + 4.77\ X_2X_4 + 12.0\ X_3X_4 - 15.92X_1^2 - 0.04X_2^2 - 34905.33X_3^2 - 0.01\ X_4^2$$

In the optimization process, the responses can be simply related to the chosen factors by linear or quadratic models. In this study, 29 experiments were performed in randomized order. The adequacy of the proposed model is then revealed using the diagnostic tests provided by ANOVA. The property of the fit polynomial model is represented by the coefficient of determination R^2. The R^2 values assure a measure of how variability in the observed response values can be

TABLE I
Instrumental Operating Conditions of AAnalyst 800 ETAAS

Steps	Temp. (°C)	Ramp Time (s)	Hold Time (s)
Dry 1	110	1	30
Dry 2	130	15	30
Pyrolysis	850	10	20
Atomization	1600	0	5
Clean-out	2450	1	3

Wavelength (λ)	283.3 nm
Hollow cathode lamp current	440.0 mA
Background correction	Zeeman-effect
Injection volume	20 µL
Slit width	0.7 nm

TABLE II
Box–Behnken Design and Observed Responses of Pb(II) Levels on Clay (mg g^{-1})

Run	pH X_1	Contact Time X_2 (min)	Adsorbent Dosage X_3 (g)	Agitation Speed X_4 (mL)	Pb(II) (qe, mg g^{-1}) Observed
1	3	31	0.075	50	8.2
2	5	60	0.05	100	85.6
3	5	31	0.1	50	49.4
4	5	2	0.075	50	45.8
5	5	2	0.1	100	27.5
6	5	31	0.075	100	121.2
7	7	31	0.075	50	47.4
8	7	31	0.05	100	54.8
9	5	60	0.075	150	80.1
10	5	31	0.05	150	61.2
11	5	31	0.075	100	120
12	5	60	0.075	50	69.8
13	5	31	0.075	100	116.9
14	5	31	0.075	100	117.2
15	5	31	0.075	100	115.9
16	3	60	0.075	100	12.1
17	7	60	0.075	100	62.6
18	5	2	0.075	150	28.4
19	5	31	0.1	150	75.5
20	3	31	0.05	100	22.7
21	5	2	0.05	100	54.3
22	7	31	0.075	150	33.2
23	5	31	0.05	50	95.1
24	3	2	0.075	100	6.7
25	3	31	0.075	150	17.5
26	5	60	0.1	100	82.2
27	7	2	0.075	100	8.3
28	3	31	0.1	100	15.1
29	7	31	0.1	100	34.3

clarified by experimental factors and their interactions (39). These analyses are performed by the agency of Fisher's 'F'-test and the P-value (probability). Based on the experimental data obtained, the levels of the three main parameters investigated in this study are listed in Table III.

RESULTS AND DISCUSSION

Characterization Method

The morphology of clay and the Pb(II)-loaded clay were characterized using a digital scanning electron microscope (SEM) coupled with an energy dispersive X-ray (EDX) (Hitachi SU3500, Japan). The spectra were recorded using a FTIR spectrophotometer (Thermo Nicolet iS10, Thermo Scientific, USA) in the frequency range from 4000 cm^{-1} to 500 cm^{-1}. The samples were analyzed with attenuated total reflectance (ATR).

FTIR Spectroscopy

The FTIR measurements were used in order to confirm the formation of Pb(II) on the clay surface. The spectra were recorded in the frequency range of 4000-500 cm^{-1}. The instrumental operating conditions are given in the table below. The FTIR spectra of the unloaded Pb(II) and the loaded Pb(II) were performed for a better comprehension of the structure. An absorption band revealing the vibrational properties of skeletal vibration of the C–O bond was observed for around 960-1030 cm^{-1}. This band is mainly assigned to the stretching vibrations of Pb–O. The natural clay sample showed lower intensity peaks at 3600 cm^{-1}, 3400 cm^{-1}, 1370 cm^{-1}, and 1242 cm^{-1} compared with the Pb(II)-loaded clay sample, suggesting a disruption of some of these groups during treatment. At around 3336 cm^{-1} peak represents the –OH group, indicating existence of the hydroxyl groups on the surface of the clay. It can be explained by some atmospheric water adsorption appearing during the FTIR measurements. Also, the C-O stretching mode of the functional groups on the surface of the clay or arising from the absorption of atmospheric CO_2 on the surface of the clay can cause peaks between 1500 and 1650 cm^{-1}. The two peaks at 2919 and 2850 cm^{-1} correspond to the C–H stretch vibration, originating from the surface of the clay, Figure 1(b), which are obviously weak in Figure 1(a), and sug-

Table of Instrumental Parameters for FTIR Analysis

Wavelength range	4000–500 cm^{-1}
Sample to KBr mass ratio	1:100
Spectral resolution	4 cm^{-1}
Crystal Type	Diamond

TABLE III
Analysis of Variance (ANOVA) for the Quadratic Polynomial Mode

Source	Sum of Squares	df	Mean Square	F Value	p-value Prob > F	
Model	39466.16	14	2819.01	283.46	< 0.0001	Significant
A-pH	2088.24	1	2088.24	209.98	< 0.0001	
B-Contact time	4084.83	1	4084.83	410.74	< 0.0001	
C-Adsorbent dosage	670.51	1	670.51	67.42	< 0.0001	
D-Agitation speed	32.67	1	32.67	3.29	0.0914	
AB	597.80	1	597.80	60.11	< 0.0001	
AC	41.60	1	41.60	4.18	0.0601	
AD	138.06	1	138.06	13.88	0.0023	
BC	136.89	1	136.89	13.76	0.0023	
BD	191.82	1	191.82	19.29	0.0006	
CD	900.00	1	900.00	90.50	< 0.0001	
A2	26291.92	1	26291.92	2643.74	< 0.0001	
B2	7324.44	1	7324.44	736.50	< 0.0001	
C2	3087.12	1	3087.12	310.42	< 0.0001	
D2	4933.39	1	4933.39	496.07	< 0.0001	
Residual	139.23	14	9.94			
Lack of Fit	119.02	10	11.90	2.36	0.2122	Not significant
Pure Error	20.21	4	5.05			
Cor Total	39605.39	28				
R-Squared	0.9965					
Adj R-Squared	0.9930					
Pred R-Squared	0.9819					

*p<0.01 highly significant; 0.01<p<0.05 significant; p>0.05 not significant.

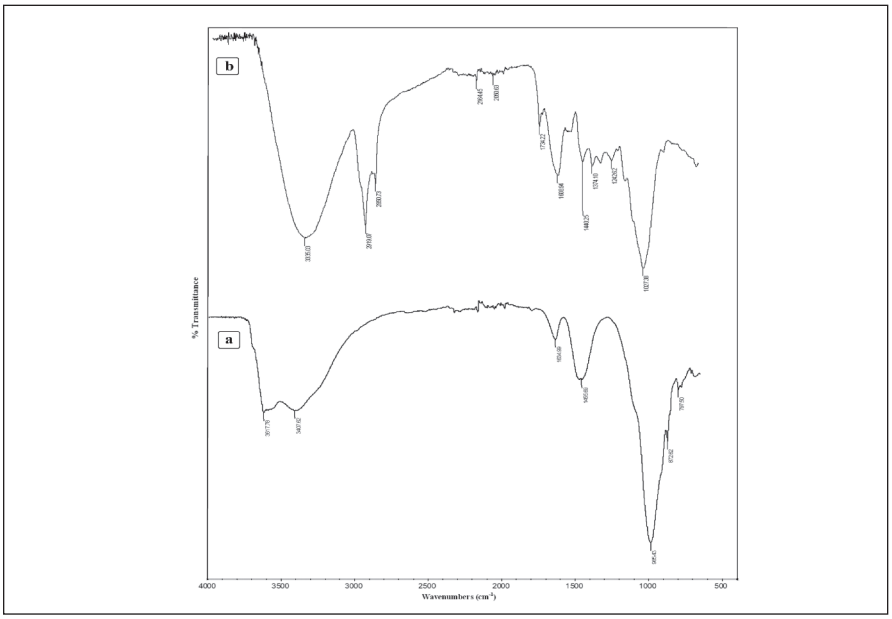

Fig. 1. FTIR spectra of (a) clay and (b) Pb-loaded clay.

gests that the surface of the clay was covered with Pb(II).

Surface Morphology

The morphological differences between the clay and the Pb(II)-loaded clay were proved by using SEM. In Figure 2, the SEM images show the differences between the surface morphologies of the clay (Figure 2a) and the Pb(II) loaded (Figure 2b). After pretreatment with Pb(II), the surface of the clay is smoother which may be due to the Pb(II) adsorption onto clay. It can be stated that the nature of this clay is good for adsorption of Pb(II).

The mineralogical composition using EDX was determined as; 21.7% for SiO_2, 6.8% for Al_2O_3, 4.8%

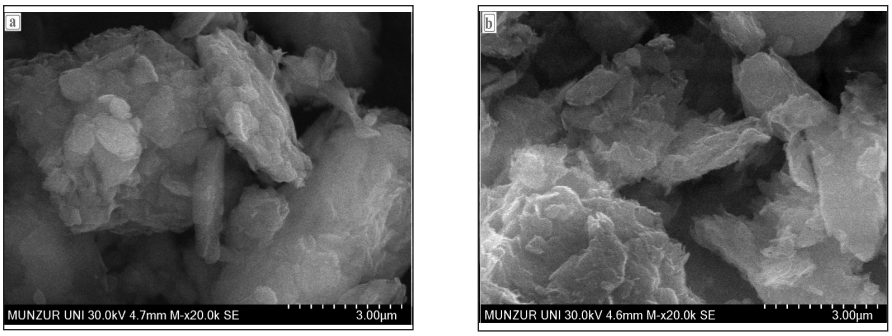

Fig. 2. SEM image of clay: (left) before adsorption of Pb and (right) after adsorption of Pb.

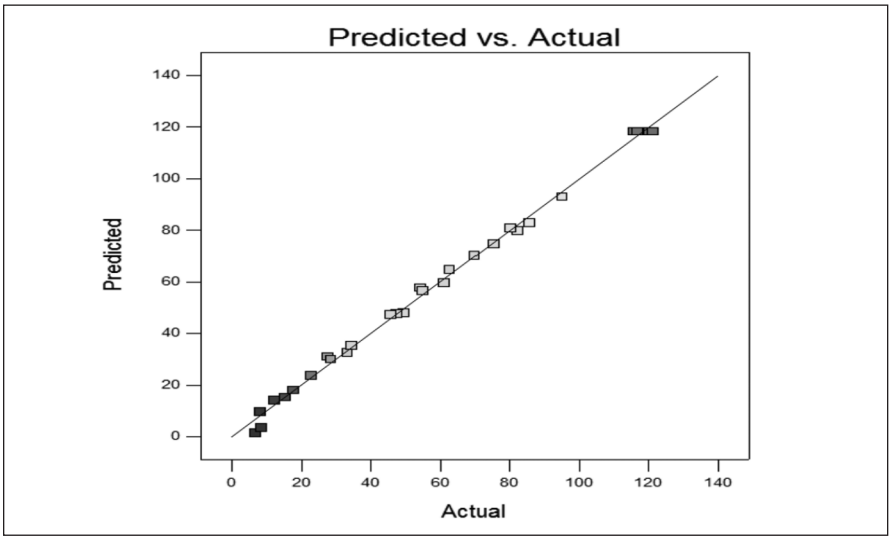

Fig. 3. Actual predicted and residual values of the experimental design.

for Fe_2O_3, 3.3% for MgO, 1.1% for K_2O, and 1.6% for CaO_2.

Second-order Polynomial Model

The results of the Pb(II) adsorption onto clay conditions using BBD with RSM and ANOVA are shown in Tables II and III, respectively. The Model F-value of 283.46 indicates that the model is significant. There is only a 0.01% chance that an F-value this large could occur because of noise. Since the "Prob>F" values are less than 0.0500, this indicates that the model terms are significant. In this case, X_1, X_2, X_3, X_1X_2, X_1X_4, X_2X_3, X_2X_4, X_3X_4, X_1^2, X_2^2, X_3^2, X_4^2 are statistically significant. On the other hand, the X_4 and X_1X_3 values greater than 0.1000 indicate that the model terms are not significant. Because the model coefficient (R^2) was 0.9965, it can be said that 99.65% of the model-predicted values (Figure 3) matched the experimental adsorbed Pb(II) values on clay. In addition, Ince and Kaplan Ince (39) reported that a model is adequate at R^2>0.75 value. The "Pred R-Squared" value of 0.9819 is in reasonable agreement with the "Adj R-Squared" of 0.9930; i.e., the difference is less than 0.2. "Adeq Precision" measures the signal-to-noise ratio and where a value greater than 4 is desirable. Thus, this study ratio of 51.448 indicates an adequate signal. This study also revealed that the lack of fit that measures the fitness of the model was not significant (p>0.05). The "Lack of Fit F-value" of 0.2122 implies that the Lack of Fit is not significant relative to the pure error. There is a 21.22% chance that a "Lack of Fit F-value" this large could occur because of noise. In addition, the number of experiments made was sufficient to determine the effects of the independent variables for Pb(II) adsorption on clay. The results verify that the statistical model was adequate in predicting the Pb(II) levels and was fitted to the second-order polynomial equation. Thus, while X_1, X_2, X_3, X_4, X_2X_3, X_3X_4, X_1^2, X_2^2, X_3^2, X_4^2 are highly significant ($p<0.01$) X_1X_2, X_1X_3, X_1X_4, X_2X_4, they are significant model terms for Pb(II) adsorption onto clay.

RSM Analysis

Two-dimensional (2D) contour plots and three-dimensional (3D) response surface graphs were made because they are useful in determining the maximum, minimum, and middle response points. Contour plots indicate the level of the variables and contribute to a desired response. Figure 4 shows the effect of contact time and pH on Pb(II) adsorption on clay. It was found that the adsorbed Pb(II) amount ($p<0.01$) increased with an increase in pH and reached a plateau at 5 (see Figure 5) and also the quadratic variables had significant effects (pH, $p<0.01$). The effects of agitatation speed and pH on Pb(II) adsorption onto clay are shown in Figure 6. The adsorbed Pb(II) amount increased with increasing adsorbent dosage until reaching a plateau at 0.075 g along with contact time reaching a plateau at 38.9 minutes. Interaction of these two variables had a significant effect on Pb(II) adsorption and also the quadratic variables had significant effects ($p<0.01$). Based on the agitiation speed up to 100 rpm and contact time studies, these two variables have important effects for Pb(II) adsorption on clay, and also on the quadratic variables ($p<0.01$).

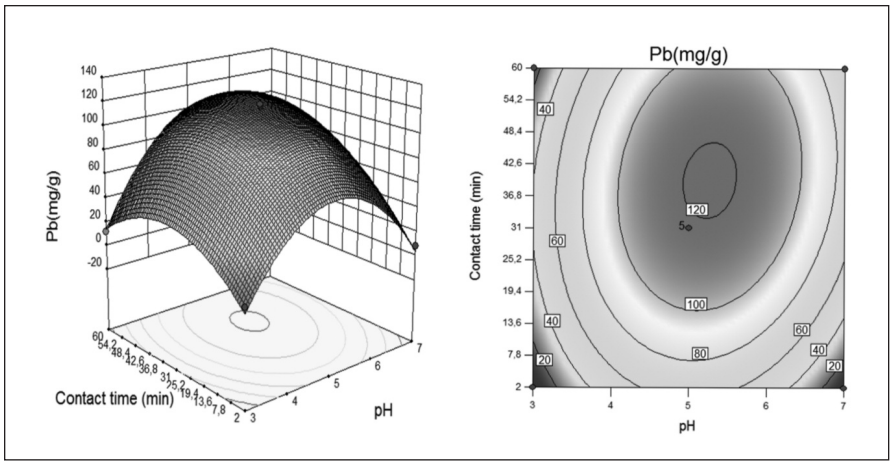

Fig, 4. Response surface and contour plot for lead adsorption on clay as contact time and pH.

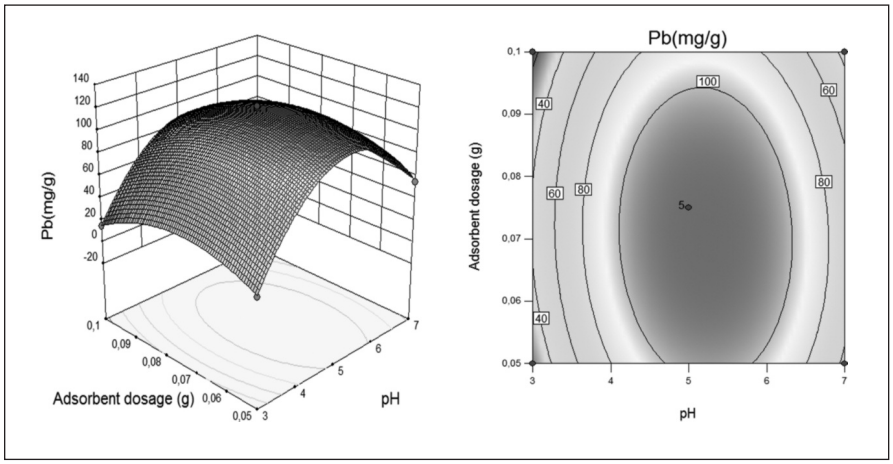

Fig. 5. Response surface and contour plot for lead adsorption on clay as adsorbent dosage and pH.

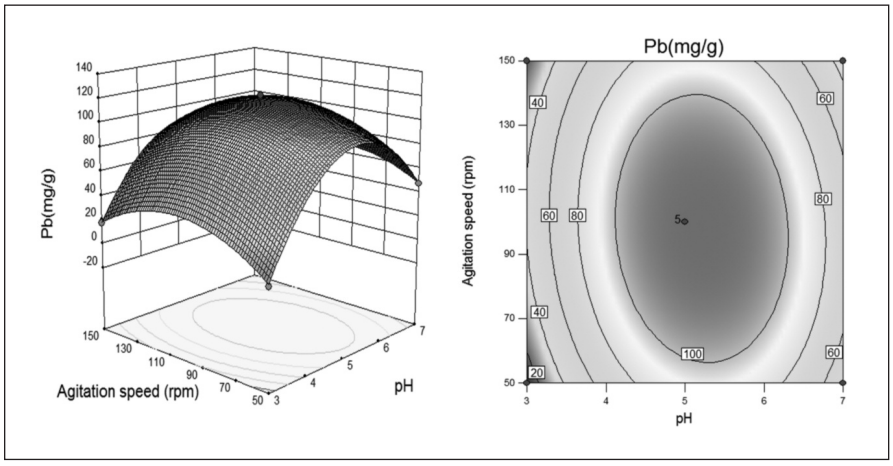

Fig. 6. Response surface and contour plot for lead adsorption on clay as agitation speed and pH.

Thus, the variables of agitation speed, pH, and dosage amount have significant effects on Pb(II) adsorption.

Confirmation Experiments

To support the optimized data given by numerical modeling, the experiments were conducted using pH 5.3, contact time 38.9 minutes, adsorbent dose 0.071 g, agitation speed 98.7 rpm, resulting in the removal of Pb(II) close to 100% (Table IV). A recent study by Ince et al. (40) reported the use of various adsorbents reported, using a 3-factor, 3-level BBD combined with RSM for maximizing Cu(II) removal from aqueous solution for adsorption of Cu(II) onto banana peel, chestnut shell, and tea leaf waste. The equilibrium data agreed well with the two isotherm models Freundlich and Langmiur. Based on the astragalus adsorption capacity results, their capacity was calculated as 1.94 mg g^{-1}, 2.25 mg g^{-1}, and 3.36 mg g^{-1} (pH 4-6), respectively. Srivastava et al. (41) removed the Cd^{2+}, Ni^{2+}, and Zn^{2+} ions from aqueous solutions of rice husk ash using Taguchi's optimization methodology. Some adsorption parameters including initial metal concentration, temperature, solution pH, adsorbent amount and stirring time were varied at three levels. The results revealed that Taguchi's method is suitable for optimizing the experiments for total metal ion removal. They obtained optimum adsorptive removal of metal ion conditions as C, i = 0–100 mg L^{-1}, T=40 °C, pH=6, m= 10 g L^{-1} and t = 60 min. Sardelle et al. (42) prepared various materials as adsorbent, including grape stalk and pomace to remove Pb and Cd. Adsorbents were characterized by BET and FTIR. They mentioned that the Langmuir and Freundlich models were fitted for Pb and Cd on these adsorbents. Optimum pH was obtained for Pb and Cd as 5.5 and 6, respectively. When grape

TABLE IV
Removal of Pb(II) Ions Using Clay From Various Alcoholic Beverage Samples

		Pb(II) (μg L^{-1})	
Sample	SA	Found	(%)Removal
Beer 1	0.0	8.3±0.4	
	20	27.9±0.4	99.0
Beer 2	0.0	6.5±0.2	
	20	26.3±0.6	99.0
Beer 3	0.0	7.6±0.2	
	20	26.8±0.3	97.0
Beer 4	0.0	7.2±0.2	
	20	26.9±0.3	99.0
Beer 5	0.0	8.1±0.3	
	20	27.8±0.3	96.0
Beer 6	0.0	9.2±0.2	
	20	28.9±0.5	97.0
Beer 7	0.0	8.8±0.4	
	20	29.0±0.6	100
Beer 8	0.0	8.7±0.2	
	20	28.8±0.5	100
Beer 9	0.0	7.7±0.2	
	20	27.7±0.2	100
Beer 10	0.0	7.7±0.2	
	10	26.6±0.4	96.0
Home-made red wine 1	0.0	17.7±0.3	
	20	38.1±2.1	100
Home-made red wine 2	0.0	21.2±3.1	
	20	41.8±2.5	100
Home-made white wine 1	0.0	28.4±1.2	
	20	49.3±2.2	100
Home-made white wine 2	0.0	23.4±2.4	
	20	42.6±2.2	100
Standard reference materials	100.0	98.0±3	99.0

SA: Standard Addition.

pomace-activated carbons were used as adsorbent removal, the gain was around 98% (41). Mishra and Patel (15) used kaolin and bentonite clays as adsorbent with a particle size between 100 mesh and 200 mesh to remove the Pb and Zn ions from water. They investigated the effect of contact time, pH, and adsorbent dosage on Pb and Zn removal. While the equilibrium time was found to be 3 hours for kaolin and bentonite, the most effective pH value for Pb and Zn removal was 6. According to experimental results, it was found that bentonite clay was an effective adsorbent for Pb and Zn removal. Potgieter et al. (43) removed Pb, Ni, Cr, and Cu from aqueous solution of palygorskite clay. Their study was carried out at room temperature and metals adsorption onto clay was studied by using a batch method, and the adsorption results were fitted to both the Langmuir and Freundlich models. The adsorption capacity of the palygorskite clay was calculated according to the Langmuir isotherm with 62.1 mg g^{-1} Pb(II), 33.4 mg g^{-1} Ni(II) g^{-1}, 58.5 mg g^{-1} Cr(VI), and 30.7 mg g^{-1} Cu(II) at a pH of 7.0 at 25 ºC (42). Ince et al. (44) studied a batch experimental system for removal of several heavy metals including Ni^{2+}, Pb^{2+}, and Cd^{2+} using banana peel food waste. After investigating the effects of various parameters, the maximum adsorbent amount was found to be Pb 0.1 g, for Cd and Ni 0.25 g. According to the results of another study (45) in an aqueous system, eggshell was used as adsorbent to remove Cd^{2+}. In that study, the design experimental methodology and RSM were used to optimize the parameters such as pH and adsorbent dosage. The RSM indicated that the optimum adsorbent dosage of hydroxyapatite was 0.57 g for the adsorption of Cd^{2+}.

Analytical Application to Real Samples

The Pb content was tested using real samples, such as beer and wine, purchased at different local markets in Tunceli city, Turkey. The Pb(II) ions were concentrated by using an adsorption technique on natural clay and determined by ETAAS. The developed analytical method of BBD combined with RSM and quadratic programming using natural clay was found to be an effective and eco-friendly adsorbent. Under optimum conditions, an approximate 50 mL of real samples was filtered and adjusted to pH 5.3. Additional 50 mL aliquots were spiked with Pb(II) at pH 5.3. The solutions were agitated with 0.071 g of clay for 38.9 minutes. The metal ions were then eluted with 4 mL of 1M HNO_3 and the Pb concentrations determined by ETAAS. The

results in Table IV show the efficiency of clay for the removal of Pb(II) ions. The results revealed that Pb concentration in the beer and wine samples were in the range of 6.5±0.2–9.2±0.2 ng mL^{-1} and 17.7±0.2–28.4±1.2 ng mL^{-1}, respectively. Accuracy of the method was studied using standard addition for the standard reference material (SRM) SPS-SW1 Batch 113 Surface Waters (Spectrapure Standards AS-Oslo, Norway), resulting in 99%.

CONCLUSION

The present study revealed that the effects of solution pH, contact time, adsorption amount, and agitation speed were researched using RSM and BBD for the adsorption of Pb(II) from alcoholic beverages by clay. The application of the present technique to alcoholic beverages is unique in the literature. The result is that the environmentally friendly adsorbent, clay, can be efficiently and simply used to remove Pb(II). Also, the obtained data from this study revealed that the removal of Pb(II) using clay was influenced by the main and quadratic independent variables effects investigated. Based on the ANOVA, whole coefficients (R^2>0.9965) were of high value in the regression model. Hence, to describe and predict the variation of the response variables, an empirical point of view was developed. In this study, optimization with BBD has the advantages of being economical, saves analysis time, and is efficient.

Received February 1, 2018.

REFERENCES

1. S.M. Al-Garni, Water SA. 31(3), 345 (2005).
2. R.H.S.F. Vieira and B. Volesky, Int. Microbiol. 3(1), 17 (2000).
3. A.H. Sulaymon, B.A. Abid and J.A. Al-Najar, Chem. Eng. J. 155(3), 647 (2009).
4. N. Ahalya, T.V. Ramachandra, and R.D. Kanamadi, Res. J. Chem. Environ. 7(4), 71 (2003).
5. J. Nouri, B. Lorestani, N. Yousefi, N. Khorasani, A.H. Hasani, S. Seif and M. Cheraghi, Environ. Earth Sci. 62(3), 639 (2011).
6. R. Jalali, H. Ghafourian, Y. Asef, S.J. Davarpanah and S. Sepehr, J. Hazard. Mater. 92, 253 (2002).
7. K. Conrad and H.C.Bruun Hansen, Bioresour. Technol. 98(1), 89 (2007).
8. F. Fu and Q. Wang, J. Environ. Manage. 92, 407 (2011).
9. M.A. Barakat, Arab. J. Chem. 4, 361 (2011).
10. M. Ahmaruzzaman, Adv. Colloid Interface Sci. 166(1-2), 36 (2011).
11. L. Yan-Hui, Z. Yanqiu, Z. Yimin, W. Dehai and L. Zhaokun, Diam. Relat. Mat. 15, 90 (2006).
12. V.K. Gupta, S. Agarwal and T.A. Saleh, J. Hazard. Mater. 185(1), 17 (2011).
13. W. Qiu and Y. Zheng, Chem. Eng. J. 145, 483 (2009).
14. K.G. Sreejalekshmi, K.A. Krishnan and T.S. Anirudhan, J. Hazard. Mater. 161(2-3), 1506 (2009).
15. P.C. Mishra and R.K. Patel, J. Hazard. Mater. 168(1), 319 (2009).
16. S.H. Lin, S.L. Lai and H.G. Leu, J. Hazard. Mater. 76(1), 139 (2000).
17. B. Bayat, J. Hazard. Mater. B95, 251 (2002).
18. M. Bernardo, S. Mendes, N. Lapa, M. Gonçalves, B. Mendes, F. Pinto, H. Lopes and I. Fonseca, J. Colloid Interface Sci. 409, 158 (2013).
19. M.A.P. Cechinel, S.M.A.G.U. de Souza and A.A.U. de Souza, J Clean Prod. 65, 342 (2014).
20. M.A. Salam, Colloids Surf. A: Physicochem. Eng. Asp. 419, 69 (2013).
21. L. Jiang, P. Liu and S. Zhao, Colloids Surf. A-Physicochem. Eng. Asp. 470, 31 (2015).
22. S. Duan, R. Tang, Z. Xue, X. Zhang, Y. Zhao, W. Zhang, J. Zhang, B. Wang, S. Zeng and D. Sun, Colloids Surf. A-Physicochem. Eng. Asp. 469, 211 (2015).
23. S. Rahimi, R.M. Moattari, L. Rajabi and A.A. Derakhshan, Colloids Surf. A-Physicochem. Eng. Asp. 484, 216 (2015).
24. S.-N. Su, H.-L. Nie, L.-M. Zhu and T.-X. Chen, Bioresour. Technol. 100, 2336 (2009).
25. K. Yetilmezsoy, S. Demirel and R.J. Vanderbei, J. Hazard. Mater. 171(1-3), 551 (2009).
26. T. Sahan and D. Özturk, Clean Techn. Environ. Policy. 16(5), 819 (2014).
27. O. Freitas, C. Delerue-Matos and R. Boaventura, J. Hazard. Mater. 167(1-3), 449 (2009).
28. F.J. Cerino Córdova, A.M. García León, R.B. Garcia Reyes, M.T. Garza González, E. Soto Regalado, M.N. Sánchez González and I. Quezada López, Int. J. Environ. Sci. Tech. 8(4), 695 (2011).
29. A. Murugesan, T. Vidhyadevi, S.S. Kalaivani, K.V. Thiruvengadaravi, L. Ravikumar, C.D. Anuradha and S. Sivanesan, Journal of Water Process Engineering 3, 132 (2014).
30. F.J. Cerino-Córdova, A.M. García-León, E. Soto-Regalado, M.N. Sánchez-González, T. Lozano-Ramírez, B.C. García-Avalos and J.A. Loredo-Medrano, J. Environ. Managmt. 95, S77 (2012).
31. M.M. Ba-Abbad, P.V. Chai, M.S. Takriff, A. Benamor and A.W. Mohammad, Mater. Des. 86, 948 (2015).
32. K. Rashid, K.S.K.Reddy, A.A. Shoaibi and C. Srinivasakannan, Clean Technol. Environ. Policy. 15, 1041 (2013).
33. S. Sugashini and K.M. Meera Sheriffa Begum, Clean Technol. Environ. Policy. 15(2), 293 (2013).
34. M.M.D. Zulkali, A.L. Ahmad and N.H. Norulakmal, Bioresour. Technol. 97(1), 21 (2006).

35. P. Tripathi, V.C. Srivastava and A. Kumar, Desalination 249(3), 1273 (2009).

36. D. Das and N. Das, Clean-Soil, Air, Water 39(2), 157 (2011).

37. B. Kiran and K. Thanasekaran, Ecol. Eng. 42, 232 (2012).

38. J.S. Varsihini C, D. Das and N. Das, J. Rare Earth. 32(8), 745 (2014).

39. M. Ince and O. Kaplan Ince, At. Spectrosc. 38(6), 200 (2017).

40. M. Ince, O. Kaplan Ince, E. Asam, and A. Önal, Atom Spect. 38(5), 142 (2017)

41. V.C. Srivastava, I.D. Mall, and I.M. Mishra, Chem. Eng. J. 140(1-3), 136 (2008).

42. F. Sardella, M. Gimenez, C. Navas, C. Morandi, C. Deiana, and K. Sapag, J. Environ. Chem. Eng. 3(1), 253 (2015).

43. J.H. Potgieter, S.S. Potgieter-Vermaak, and P.D. Kalibantonga, Miner. Eng. 19(5), 463 (2006).

44. M. Ince, O. Kaplan Ince, V. Yonten, and N.M. Karaaslan, At. Spectrosc. 37(3), 130 (2016).

45. O. Kaplan Ince, M. Ince, and N.M. Karaaslan, V. Yonten, Anal. Lett. 49(15), 2513 (2016).

Use of Chemometric Tools for HG-AAS Instrumental Optimization in the Determination of Se in Nuts Grown in Brazil

Anderson dos Santos Greco[a], Eliana Janet Sanjinez Argandona[b], Marcela Zanetti Corazza[a], and Jorge Luiz Raposo Jr.*[,a,c]

[a] Federal University of Grande Dourados, School of Exact and Technology Science, P.O. Box 364, 79804-970 Dourados, MS, Brazil

[b] Federal University of Grande Dourados, School of Engineering, P.O. Box 364, 79804-970 Dourados, MS, Brazil

[c] Institute of Chemistry, Federal University of Mato Grosso do Sul, P.O. Box 549, 79070-900 Campo Grande, MS, Brazil

ABSTRACT

The determination of total selenium (Se) is described in nuts such as bacuri (*Platonia insignis Mart.*), baru (*Dipteryx alata Vog.*), bocaiuva (*Acrocomia aculeata* (Jacq.) Lodd), and cashew (*Anacardium occidentale L.*) (other than the well-known Brazilian nut) using hydride generation coupled to a flame atomic absorption spectrometer (HG-AAS). The best experimental conditions to generate the volatile hydride (H_2Se) were established by multivariate statistical analysis. The conditions of the pre-reduction step to generate the Se hydride were optimized using the Pareto diagram and Doehlert design. Best results were achieved when 0.6 mol L^{-1} HCl, 1.0% (m/v) $NaBH_4$ in 0.5% (m/v) NaOH, and a 00-cm reaction coil were used. For Se determination by HG-AAS, analytical curves were built in the 0.50 - 25.0 μg L^{-1} range resulting in a linear coefficient correlation better than 0.9970. The accuracy of the sample preparation procedure and HG-AAS determination were evaluated by addition and recovery tests, and the recoveries were found in the 90.3–95.8% range with a relative standard deviation (%RSD) of < 4.7%. Using the proposed methodology, the limit of detection obtained was 0.1315 μg L^{-1} with a %RSD up to 1.9%. The Se concentrations in the samples were in the 0.515±0.017–0.657±0.029 μg g^{-1} Se range. The multivariate analysis applied to the experimental results showed to be a useful tool because it allows reducing the number of experiments (from 60 to 8) with satisfactory accuracy.

INTRODUCTION

Selenium (Se) and its related metalloid species are essential for humans and animals due to their medicinal properties (1-3), powerful antioxidant characteristics, and protectors against heavy metal toxicity (4). Due to the health-related benefits, the U.S. Food and Nutrition Board recommends 55 μg/day for adults and 70 μg/day for lactating mothers as a dietary reference intake (DRI) of selenium (5, 6). The tolerable upper intake for adults is set at 400 μg/day (6, 7).

Food is considered the most important source of Se, and poultry, beef, eggs, seafood, wheat flour, oat grains, and brown rice are the main dietary staples (8-11). In addition, species of the genus *Allium* (onion, garlic, leek, etc.) and *Brassica* (cabbage, cauliflower, broccoli, mustard, brussels, turnip, radishes, etc.) also contain small amounts of selenium (12). However, among these numerous foods that easily furnish the recommended daily intake of selenium (13), the Brazil nut (*Bertholletia excelsa*) is worldwide known and has a a high content of selenium (9, 12, 14, 15). Due to the environmental and climatic diversity in Brazil, there is an extensive variety of nuts grown. These species also deserve dedicated attention and are discussed below.

** Corresponding author.*
E-mail: jorgeluizraposo@gmail.com
Tel: +55 67 33453937

The determination of Se can be carried out through different spectrometric techniques including electrothermal atomic absorption spectrometry (ETAAS) (16-18), inductively coupled plasma mass spectrometry (ICP-MS) (19-21), inductively coupled plasma optical emission spectrometry (ICP-OES) (22, 23), hydride generation atomic absorption spectrometry (HG-AAS) (19, 24), hydride generation atomic fluorescence spectrometry (HG-FAAS) (25, 26), instrumental neutron activation analysis (8), and the hyphenated technique of HPLC-ICP-MS (27). With regard to Se speciation, hyphenated techniques are usually preferred and applied for analytical purposes (28, 29). However, these techniques result in high laboratory costs. Hydride generation coupled to an AAS is an alternative and can also produce high sensitivity and be used as an optional and satisfactory technique to determine low Se concentrations in different matrices (31, 32). In addition, the experimental parameters of HG-AAS can be successfully established by multivariate analysis, allowing ideal conditions and requiring a reduced number of experiments for the determination of hydride elements (32, 33).

Due to the lack of information about the content of Se in native nuts from midwestern Brazil, this paper reports the development of a novel method for the determination of selenium in bacuri (*Platonia insignis Mart.*), baru (*Dipteryx alata Vog.*), bocaiuva (*Acrocomia*

aculeata (Jacq.) Lodd), and cashew (*Anacardium occidentale L.*) nuts by hydride generation coupled to atomic absorption spectrometry, and using multivariate statistical analysis to establish the best conditions for the generation of H_2Se.

EXPERIMENTAL

Instrumentation

A Varian 240FS flame atomic absorption spectrometer (Agilent Technologies®, Mulgrave, Victoria, Australia), equipped with a deuterium background corrector, was used throughout this work and the instrumental operating parameters are listed in Table I. A VGA 77 Vapor Generation (Agilent Technologies) with a thermal quartz flow cell atomizer was used to generate and atomize the Se hydride. It was controlled by a peristaltic pump, and measurement of the solutions was carried out in four replicates, and the peak height (absorbance) of the blank, analytical solutions, and samples were obtained under optimum instrumental conditions (Table I). Atomization of the SeH_2 was performed using an oxidizing air-acetylene flame. High-purity acetylene (99.7%) and argon (99.999%) (White Martins®, Dourados, MS, Brazil) were used as fuel and carrier gas, respectively. A 515 Orion (Fanem®, São Paulo, SP, Brazil)

TABLE I
HG-AAS Instrumental Operating Conditions for the Determination of Se

Instrumental Conditions	Se
Working range	2.0–25.0 mg L^{-1}
Wavelength	196.0 nm
Lamp current	10 mA
Burner head	100 mm
Air flow rate	13.0 L min^{-1}
Acetylene flow rate	2.0 L min^{-1}
Argon flow rate	0.1 L min^{-1}
Slit width	1.0 nm

forced air oven and a TE-361 (Tecnal®, Piracicaba, SP, Brazil) stainless steel mill were used to dry and powder the nuts, respectively. The appropriate amount of samples was digested in a MARS 6 microwave oven (CEM Corporation, Matthews, NC, USA).

Standard Solutions and Reagents

High purity deionized water obtained from a Milli-Q® Plus reverse osmosis system (resistivity 18.2 MΩ-cm, Millipore Corporation, Bedford, MA, USA) was used to prepare all solutions. Digestion of the nuts was carried out using hydrochloric acid [37% (v/v)] and nitric acid [65% (v/v)] (Sigma-Aldrich, St. Louis, MO, USA), plus sulfuric acid [98% (m/v)] and hydrogen peroxide [30% (m/v)] (Vetec®, Duque de Caxias, RJ, Brazil).

Aqueous analytical solutions containing 0.5–25.0 μg L^{-1} Se were prepared daily using appropriate dilutions of mono-element 1000-mg L^{-1} standard stock solutions (SpecSol®, SRM-682, USA) of Se(IV) in 1.0% (v/v) nitric acid. All solutions were stored in high-density polypropylene bottles (Nalgene®, Rochester, NY, USA).

A 100 mL 1.0% (m/v) $NaBH_4$ solution [97% purity (m/m), Vetec®, Duque de Caxias, RJ, Brazil] was prepared daily in 0.5% (m/v) sodium hydroxide [99% purity (m/m), Vetec] medium and used as a reducing agent in the HG system. A 0.60 mol L^{-1} HCl solution was prepared and used as the carrier solution and during the generation of the Se hydride. To convert Se(VI) to Se(IV), a pre-reduction step was carried out using 10.0% (m/v) KI [99% purity (m/m) (Vetec), in 2.4 mol L^{-1} HCl medium.

The best experimental conditions (reaction coil, concentration of HCl carrier solution, and % (m/v) of the reducing agent) to generate the H_2Se were established by multivariate statistical analysis using working solutions containing 25.0 μg L^{-1} Se.

Plastic bottles and glassware were separated and cleaned by soaking in 10% (v/v) HNO_3 for at least 24 hours, followed by thoroughly rinsing with deionized water before use.

Sample Preparation

Samples of native bacuri, baru, bocaiuva, and cashew nuts were collected from the trees during 2015 from Bonito, Campo Grande, Dourados and Rochedo Cities (Mato Grosso do Sul, Brazil), respectively. A 1000-g amount of each nut was randomly collected, stored in individually labelled paper bags, and then transported to the laboratory. The nuts were separately and thoroughly washed with running tap water as well as with deionized water. A 5.0-g subsample of each species was dried at 50 ºC for 30 hours in a forced air oven, ground in a stainless steel mill, and then sieved using a No. 20 sieve (0.84 mm opening size). All samples were individually stored in identified plastic bags and kept under refrigeration until sample preparation.

The native nuts were mineralized using acid digestion in a closed vessel microwave oven. For this purpose, a 0.5000-g portion of pretreated bacuri, baru, bocaiuva, and cashew samples was accurately weighed (± 0.0001 g) and transferred into a 100-mL microwave flask, followed by the addition of 6.0 mL of HNO_3 and 2.0 mL of HCl. The optimized heating program used is listed in Table II. After digestion and cooling, the resulting solutions were transferred to 20-mL volumetric flasks, and the volume was completed with deionized water. Three sample and blank replicates were used for the acid decompositions.

Since the determination of Se requires only the Se(IV) oxidation

state to produce SeH_2, a pre-reduction step was performed to reduce all Se(VI) to Se(IV). Thus, after the sample preparations, 6.0-mL aliquots of the digested sample were transferred to 15-mL polyethylene bottles, followed by addition of 1.0 mL of 10% (m/v) KI and 3.0 mL HCl [37% (v/v)]. The solutions were mixed with a vortex stirrer for 10 seconds to complete homogeneity and kept at rest for 30 seconds. The procedure resulted in homogeneous and colorless solutions. All solutions were prepared in triplicate.

Optimization of HG-AAS Experimental Conditions

In order to find the optimum HG-AAS experimental conditions for SeH_2 generation in the determination of Se in the native Brazilian nuts, a 2^3 full factorial design was employed. The influence of HCl concentration, $NaBH_4$ concentration, and reaction coil length were evaluated and the maximum (+) and minimum (-) levels studied (see Table III). The experiments were randomly chosen and carried out in duplicate to avoid possible systematic errors. The significance of each factor was evaluated from the analysis of variance (ANOVA) performed at 95% confidence interval and graphically represented by a Pareto chart. For final optimization of the HCl and $NaBH_4$ concentrations, a Doehlert matrix for two variables and a response surface methodology were used. All results obtained from the multivariate analysis were processed using Statistica® software (Version 10) (TIBCO Software Inc., Palo Alto, CA, USA) at a 95% confidence level.

TABLE II
Microwave-assisted Digestion Heating Program for Nuts

Step	t_{Ramp} (min)	t_{Hold} (min)	Power (W)	T (°C)
1	5	5	1000	85
2	7	5	1000	120
3	11	13	1000	200
3	0	20	0	30 (Ventilation)

TABLE III
Factors Studied in 2^3 Full Factorial Design, Levels, and Analytical Responses

Factor			Level	
			Low (-)	High (+)
HCl (mol L^{-1})			1.0	5.0
$NaBH_4$ (%)			0.15	1.5
Reaction Coil Length (cm)			30	100
Experiment	HCl	$NaBH_4$	Coil Length	Absorbance Sb(IV) (Peak Height)
1	-	-	-	0.253/0.256
2	+	-	-	0.311/0.317
3	-	+	-	0.427/0.418
4	+	+	-	0.502/0.505
5	-	-	+	0.285/0.273
6	+	-	+	0.387/0.387
7	-	+	+	0.508/0.506
8	+	+	+	0.549/0.534

Analytical Measurements

Standards, samples (bacuri, baru, bocaiuva, and cashew), carrier (HCl), and a reduction ($NaBH_4$) solution were pumped into the HG gas/liquid separator system using three Tygon® tubes with a 1.00-mm i.d. For SeH_2 generation, the aspiration rates of the sample/standards, carrier and reduction solutions were 8.0, 1.0, and 1.0 mL min^{-1}, respectively. A 0.6 mol L^{-1} HCl and a 1.0% (m/v) $NaBH_4$ in 0.5% (m/v) NaOH solution were used for Se(IV) determination. The reagents were mixed with the standard solutions or samples by dispersion in the 100-cm reaction coil at 1.0 mm i.d. to generate SeH_2. The hydrogen selenide was conducted into a 17-cm cell T-type quartz insert on the AAS burner at a 100-mL min^{-1} argon flow rate (99.999%, White Martins®, Dourados, MS, Brazil). The measurements were performed at the main atomic line for Se (196.0 nm) using an oxidizing air-acetylene flame (see Table I) to atomize Se, and its determination was carried out within 2.0–25.0 μg L^{-1} intervals of the calibration curves.

The accuracy was evaluated by recovery tests using all samples spiked with 3.00 and 6.00 μg L^{-1} Se(IV), which corresponds to 0.300 and 0.600 μg g^{-1} Se, respectively. The precision of the method was checked by means of calculating the relative standard deviation (%RSD) of the sample measurements. The limits of detection (LOD) and quantification (LOQ) for Se were calculated according to the IUPAC recommendations (34).

RESULTS AND DISCUSSION

HG-AAS Instrumental Optimization Using Multivariate Analysis

The influence of the most important factors for the selenium generation step, which involved hydrochloric acid concentration as a carrier solution, concentration of the

reducing agent (sodium tetradydroborate – $NaBH_4$) and a reaction coil length using a 25 µg L^{-1} Se(IV) standard solution, was studied by means of a 2^3 full factorial design. Table III shows the analytical responses for each assay and the results were analyzed through a Pareto chart (Figure 1) where all studied variables and one of the interactions were statistically significant at the 95% confidence interval. Among the studied factors, the $NaBH_4$ concentration proved to be a most significant positive effect (65.664). This demonstrates clearly that an increase on the $NaBH_4$ concentration provides improvements on the hydride generation due to a reduction of Se(IV) to H_2Se in a strongly acidic medium. The NaOH concentration in the reduction solution [0.5%, (m/v)] does not have to be optimized since NaOH is only added to the reducting agent in order to stabilize the $NaBH_4$ in the solution (35). It is important to emphasize that the working solutions of $NaBH_4$ in the alkaline medium were prepared daily and minutes before starting analysis due to the degradation of the $NaBH_4$ caused by an increase in the evolution of the hydrogen from the hydrolysis of BH_4^- (36). The pump flow rate of the reduction solution was fixed at 1.0 mL min^{-1}.

The hydrochloric acid concentration, which is the second most important factor in Se determination, demonstrated a strong influence on the hydride generation with a positive effect (25,112) since the presence of protons in the reaction is essential to form the Se(IV) hydride (35, 37). In addition, in samples containing high OH^- concentration, the HCl concentration is necessary to neutralize the sample and to react with the reducing agent and the analytes. The pump flow rate of the hydrochloric acid as a carrier solution was fixed at 1.0 mL min^{-1}. Although the factors of $NaBH_4$ and HCl concentrations have presented a positive effect when analyzed individually, its interaction of 1*by*2 (HCl*by*$NaBH_4$) showed a negative effect, indicating an antagonistic effect of both of these factors on the Se(IV) determination. This implies that better results in the Se(IV) determination are obtained when one of the factors is at its highest level while the other is at its lowest, as studied within the experimental domain.

Using 1.0 mL min^{-1} for the carrier solution and reducing agent, and 8.0 mL min^{-1} for the Se(IV) standard flow rates, the 100 cm reaction coil length was the third most significant factor. The positive effect on the Se(IV) hydride determination due to the higher reaction time with the carrier gas, the reducing agent, and the Se(IV) species before reaching the optical pathway was observed. Thus, a reaction coil of 100 cm was chosen for all studies. Although this factor proved to be a significant factor when analyzed independently (see Figure 1), their interactions with other factors, such as reducing agent ($NaBH_4$) and carrier gas (HCl), were not significant at the 95% confidence interval.

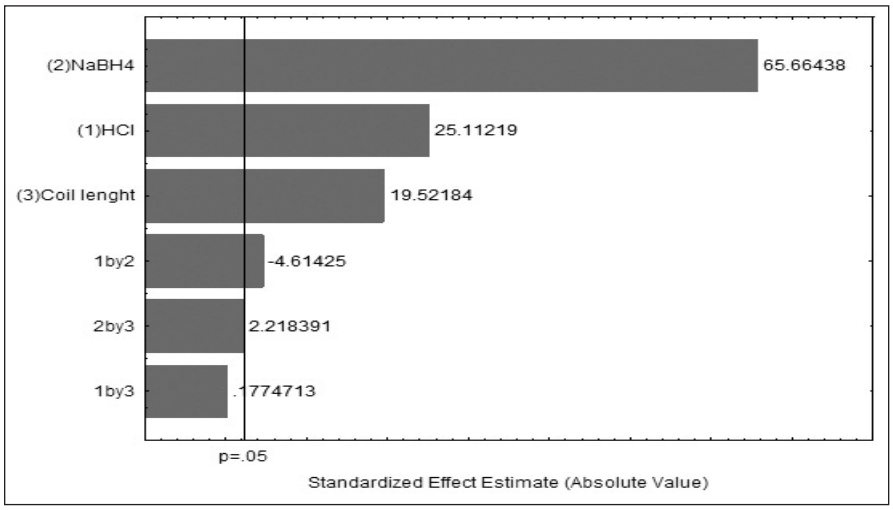

Fig. 1. Pareto's Chart obtained from the 2^3 full factorial design for the determination of Se by HG-AAS.

Therefore, according to the achieved results and considering that during the assays with the $NaBH_4$ concentration at its highest level, a decrease in precision of the results (%RSD) was observed most likely due to the very violent reaction under these conditions. For this reason, a Doehlert matrix (Table IV) with triplicate at the central point was used for obtaining the optimum values for the reducing agent ($NaBH_4$) and carrier solution (HCl). From the Doehlert design, the quadratic model, which establishes the relationship between the two factors and the analytical response (absorbance as peak height), was obtained. The model was described according to the following equation:
$Abs = -0.505 (\pm 0.016) + 0.522RA (\pm 0.018) - 0.284RA^2 (\pm 0.007) + 3.014CS (\pm 0.044) - 2.574CS^2 (\pm 0.038) + 0.077RAxCS (\pm 0.021)$.
According to ANOVA, the obtained $F_{calculated}$ (6.737) was lower than $Ft_{abulated}$ (18.51) at the 95% confidence interval, which confirms the absence of lack of fit and demonstrates that the regression model is considered to be an accurate representation of the experimental data. In addition, the high determination coefficient ($R^2 = 0.99904$) also points out that the quadratic model fits

very well to the experimental results. Using the quadratic model, the response surface was constructed, showing a maximum point at the $NaBH_4$ concentration of 1.00% and HCl concentration of 0.60 mol L^{-1} (Figure 2). These values were further used as the best conditions for determining the analytical features of the developed method. Validation of the model also has been performed by replacing RA (reducing agent) and CS (carrier solution) with the optimum values obtained. The predicted values by the quadratic model are very close to that obtained experimentally, which means that the model can be used to predict the response in all experimental domains (Table IV).

Analytical Features of HG-AAS for the Determination of Se

The only way to generate the SeH_2 species is from ionic tetravalent selenium (selenite) (35, 38). Since Se has other oxidation forms [e.g., Se(VI)], the reduction step must be performed to produce the desired species of Se. The reduction procedure is commonly carried out by adding a reducing agent and concentrated HCl into the selected digested sample solution volume (6). Moreover, the efficiency of the Se determination by HG-AAS depends on the time between the reduction step and hydride generation (35, 38). According to literature (6), satisfactory recoveries are obtained if Se hydride generation is carried out immediately after the reduction. It should be noted that by increasing the time between reducing step and analysis, problems related to a back-oxidation of Se(IV) to Se(VI) by chlorine gas formed in the reduction process have been reported (32). In this work, the pre-reduction step of Se(VI) to Se(IV) was evaluated using 6.0 mL of digested sample, 1.0 mL of 10% (m/v) KI, 3.0 mL HCl [37% (v/v)], and an aliquot of 150 µL of 1000 µg L^{-1} Se(VI) standard solution in order to contain 10.0 µg L^{-1} Se. The solution was completed to 15 mL with high purity deionized water and vortex-stirred for 10 seconds. Homogeneity of the solutions was obtained after 30 seconds; in other words, it was satisfactory and is enough time to convert the Se(VI) to Se(IV). Recoveries of 94.0 ± 2.0% indicates that this pre-reduction step, followed by HG-AAS analysis, is satisfactory to reduce Se(VI) to Se(IV). Besides, this pre-reduction step was evaluated day-to-day and no variations were observed between them at the 95% confidence level (Student's *t*-test).

Under the optimum conditions established for the pre-reduction step and by multivariate analysis for Se hydride generation, analytical curves were built in the 0.50–25.00 µg L^{-1} interval for Se(IV). Typical linear correlation coefficients better than 0.9970 were constantly obtained and the limits of detection (LOD) and quantification (LOQ), defined as three times and ten times, respectively, of the standard

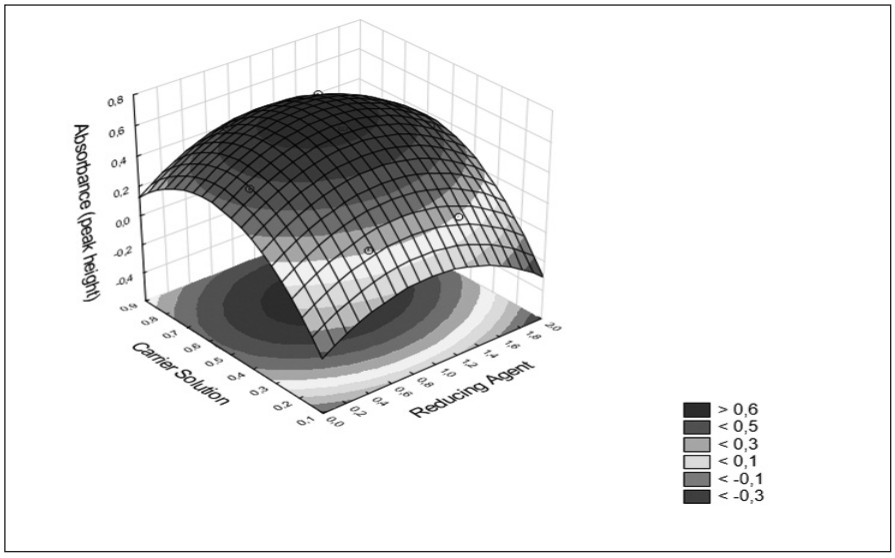

Fig. 2. Response surface for $NaBH_4$ [% (m/v)] and HCl (mol L^{-1}) concentrations.

TABLE IV
Doehlert Matrix Design Used for Optimizing Reducing Agent ($NaBH_4$) and Carrier Solution (HCl) in the Determination of Se for HG-AAS

Experiment	Factors		Absorbance (Peak Area)	Predicted Values by Quadratic Model
	Reducing Agent (%, m/v)	Carrier Solution (mol L^{-1})		
1	1 (0)	0.5 (0)	0.640	0.635
2	1 (0)	0.5 (0)	0.636	0.635
3	1 (0)	0.5 (0)	0.630	0.635
4	1.8 (1)	0.5 (0)	0.442	0.447
5	1.4 (0.5)	0.8 (0.866)	0.525	0.520
6	0.2 (-1)	0.5 (0)	0.465	0.460
7	0.6 (-0.5)	0.2 (-0.866)	0.210	0.215
8	1.4 (0.5)	0.2 (-0.866)	0.196	0.191
9	0.6 (-0.5)	0.8 (0.866)	0.502	0.507

The number between parentheses represents the Doehlert matrix coded values.

deviation of 12 measurements of a blank, divided by the slope of the calibration curve, were 0.13 and 0.44 μg L^{-1}, respectively. However, since the results for the determination of Se in native nuts are expressed as μg g^{-1}, the limits of detection and quantification were converted to this order and the values are expressed as 0.013 and 0.044 μg g^{-1} Se, respectively. The precisions, which are expressed as the relative standard deviation (%RSD) for n=4, were 1.9% using the HG-AAS atomization system.

Determination of Se in Different Native Brazilian Nuts by HG-AAS

The Se concentration in nuts, as well in the most varied types of environmental samples, is in the μg g^{-1} range (12). Since the limit of detection obtained with the proposed methodology was (0.013 μg g^{-1}), it allows below μg g^{-1} determination in the native Brazilian nuts.

The accuracy of the sample preparation procedure and the determination method was evaluated using the addition/recovery tests for all samples. Different volumes of a 1.00-mg L^{-1} Se(IV) standard solution were added in order to contain 3.00 and 6.00 μg L^{-1} in the sample before starting the sample preparation procedure, representing close to 50% (0.300 μg g^{-1}) and 100% (0.600 μg g^{-1}) of natural Se concentration in the samples analyzed. The recovery values were in the 90.3–95.8% range, with the RSD in the 0.4–3.9% range (see Table V).

According to the results of the present study, the relative standard deviations (%RSD) obtained varied from 1.6–4.7%. The recovery tests show that the established methodology is suitable for the determination of Se in the selected nut samples (see Table V).

According to the U.S. Food and Nutrition Board, an amount of 55 μg/d of Se can be considered the dietary reference intake (DRI) for adults. Since the Se concentration in the selected nuts varied from 0.515 to 0.657 μg g^{-1}, the DRI can be reached by daily ingestion of 83, 106, 91, and 96 g of bacuri, baru, bocaiúva, and cashew nuts, respectively. According to the Brazilian National Health Surveillance Agency or ANVISA (Agência Nacional de Vigilância Sanitária), any food can be considered a nutritional source when 100 g provides 15% of the DRI and is considered rich in Se when it provides about 30%. It can, therefore, be stated that all nuts evaluated in this study are rich sources of Se.

TABLE V
Results (Mean ± Standard Deviation) for the HG-AAS Determination (n= 3) of Se (μg g^{-1}) in Native Brazilian Nuts

Sample	Se Added (μg g^{-1})	Se Measured (μg g^{-1})	Recovery (%)	RSD (%)
Platonia insignis Mart.	0.000	0.657 ± 0.029	-	4.7
	0.300	0.933 ± 0.005	92.0	2.2
	0.600	1.206 ± 0.008	91.5	1.5
Dipteryx alata Vog.	0.000	0.515 ± 0.017	-	4.3
	0.300	0.794 ± 0.015	93.1	1.1
	0.600	1.057 ± 0.022	90.3	0.4
Acrocomia aculeata (Jacq.) Lodd				
	0.000	0.602 ± 0.009	-	1.6
	0.300	0.879 ± 0.011	92.4	2.6
	0.600	1.177 ± 0.019	95.8	0.9
Anacardium occidentale, L.	0.000	0.568 ± 0.026	-	3.1
	0.300	0.852 ± 0.021	94.7	3.9
	0.600	1.131 ± 0.029	93.9	2.4

CONCLUSION

The use of the multivariate analysis has proven to be an outstanding tool in developing an analytical methodology for Se determination by using diluted solutions of HCl and $NaBH_4$ with HG-AAS as a detection technique. The proposed fast and robust procedure reduces Se(VI) to Se(IV) and shows good recoveries (90.3 – 95.8%). In addition, the HG-AAS technique presented limits of detection (LOD) close to 0.013 μg g^{-1} and provided an RSD better than 4.7%.

ACKNOWLEDGMENT

The authors thank the Fundação de Apoio ao Desenvolvimento do Ensino, Ciência e Tecnologia do Estado de Mato Grosso do Sul (Fundect, Process 23/200.665/2012), the Conselho Nacional de Desenvolvimento Científico e Tecnológico (CNPq, Process n. 479186/2013-8), and FINcanadora de Estudos e Projetos (FINEP, contract: 04.13.0448.00) for their financial support of this work.

Received February 14, 2018.

REFERENCES

1. B.D. Wake, A.R. Bowie, E.C. Butler and P.R. Haddad, Trac-Trend. Anal. Chem. 23, 491 (2004).
2. C.B. Hymer and, J.A. Caruso, J. Chromatogr. 1114, 1 (2006).
3. Y. Wang and L. Fu, Biol. Trace. Elem. Res. 149, 110 (2012).
4. C.W. Nogueira, G. Zeni and J.B.T. Rocha, Chem. Rev. 104, 6255 (2004).
5. P. Trumbo, A.A. Yates, S. Schlicker, and M. Poos, J. Am. Diet. Assoc. 101, 294 (2001).
6. A.S. Abdallah, I.N.B. Castilho, B. Welz, E. Carasek, I.B.G. Martens, A. Martens and S.M.F. Cozzolino, Talanta 85 1350 (2011).
7. G.F. Combs Jr., L.C. Clark and B.W. Turnbull, Bio. Factors. 14, 153 (2001).
8. P.P. Parekh, A.R. Khan, M.A. Torres and M.E. Kitto, J. Food. Comp. Anal. 21, 332 (2008).
9. M.P. Rayman, Br. J. Nutr. 100, 254 (2008).
10. B.M. Thomson, R.W. Vannoort and R.M. Haslemore, Br. J. Nutr. 99, 614 (2008).
11. EPA, http://www.epa.gov/ttnatw01/hlthef/selenium.html1, Last visited: 28/12/2016.
12. C.A. Prauchner, A importância do Selênio para a agropecuária e saúde humana, Ed. da UFSM, Santa Maria, Brazil (2014).
13. M. Tuzen, K.O. Saygi and M. Soylak, Talanta. 71, 424 (2007).
14. E. Dumont, F. Vanhaecke and R. Cornelis, Anal. Bioanal. Chem. 385, 1304 (2006).
15. M. Lemire, M. Fillion, F. Barbosa Jr., J.R.D. Guimarães and D. Mergler, Sci. Total. Environ. 408, 4076 (2010).
16. R. Sabe, R. Rubio, and L. Garcia-Beltran, Anal. Chim. Acta 419, 121 (2000).
17. A.P Oliveira, J.A.G. Neto, J.A. Nóbrega, P.R.M. Correia and P.V Oliveira, Food. Chem. 93, 355 (2005).
18. A. Bidari, E.Z. Jahromi, Y. Assadi and M.R.M.H. Hosseini, Microchem. J. 87, 6 (2007).
19. W.T. Buckley, J.J. Budac and V. David, Anal. Chem. 64, 724 (1992).
20. S.J. Santos, H. Mokudai and S. Tanaka, J. Anal. At. Spectrom. 12, 409 (1997).
21. A.S. Ribeiro, M.A. Viera and A.J. Curtius, Spectrochim. Acta. B. 59, 243 (2004).
22. P.C. Hernandez, J.F. Tyson and C. Peter, J. Anal. At. Spectrom. 22, 298 (2006).
23. P. Qiu, C. Ai, L. Lin, J. Wu and F. Y, Microchem. J. 87, 1 (2007).
24. K. Agrawal, K.S. Patel, and K. Shrivas, J. Hazard. Mater. 161, 1245 (2009).
25. P. Smrkolj and V. Stibilj, Anal. Chim. Acta. 512, 11 (2004).
26. J.B. García, M. Krachler, B. Chen and W. Shotyk, Anal. Chim. Acta 534, 255 (2005).
27. H.F. Li, E. Lombi, J.L. Stroud, S.P. Mcgrath and F.J. Zhao, J. Agr. Food. Chem. 58, 11837 (2010).
28. J.L. Capelo, C. Fernandez, B. Pedras, P. Santos, P. Gonzalez and C. Vaz, Talanta 68, 1442 (2006).
29. P. Cuderman, I. Kreft, M. Germ, M. Kovacevic and V. Stibilj, J. Agr. Food. Chem. 56, 9114 (2008).
30. M. Navarro, H. Lopez, M.L. Ruiz, S. Gonzalez, V. Perez and M.C. Lopez, Sci. Total. Environ. 175, 245 (1995).
31. P.C. Aleixo, J.D.A. Nóbrega, D. Santos Júnior and R.C.S. Müller, Quim. Nova 23, 310 (2000).
32. R.F. Teófilo and M.M. Ferreira, Quim. Nova 29, 338 (2006).
33. S.L.C. Ferreira, M.D.G.A. Korn, H.S. Ferreira, E.G.P. da Silva, R.G.O. Araújo, A.S. Souza, S.M. Macedo, D.D.C. Lima, R.M. de Jesus, F.A.C. Amorim and J.M. Bosque Sendra, Appl. Spectrosc. Rev. 42, 475 (2007).
34. L.A. Currie, Anal. Chim. Acta. 391, 105 (1999).
35. J. Dedina and D.L. Tsalev, Hydride Generation Atomic Absorption Spectrometry, John Wiley & Sons Ltd., Chichester, UK (1995).
36. N. Erta, Z. Arslan and J.F. Tyson, J. Anal. At. Spectrom. 23, 223 (2008).
37. I. Takase, H.B. Pereira, A.S. Luna, P. Grinberg and R.C. de Campos, Quím. Nova 25, 1132 (2002).
38. B. Welz and M. Sperling, Atomic Absorption Spectrometry, 3th ed., WILEY VCH Verlag GmbH, Weinheim, Germany (1999).

Fractionation of Manganese in Soil Samples Collected From the Lakhra Coal Field in Pakistan Using Two Modes of Atomic Absorption Spectrometry

Mustaqeem ur Rahman, Tasneem G. Kazi*, Huma Shaikh, and Jamshed Ali
National Centre of Excellence in Analytical Chemistry, University of Sindh, Jamshoro 76080, Pakistan

ABSTRACT

The fractionation of manganese (Mn) in soil samples of three coal mining areas was carried out using Community Bureau of References sequential extraction (BCR-SE) method. The BCR-SE provides information about extractable Mn, bound in different chemical forms such as the acid-soluble 0.11 mol L^{-1} acetic acid, the reducible fraction requires 0.1 mol L^{-1} hydroxylammonium chloride, and Mn bound with the oxidizable fraction of 8.8 mol L^{-1} requires hydrogen peroxide plus ammonium acetate (1.0 mol L^{-1}), respectively. The Lixiviation test (DIN 38414-S4) was also carried out to evaluate the leachable Mn content in all three soil samples. The total Mn in the soil samples (pseudo-total content) was determined by the digestion of the soil samples with aqua regia. The total concentration of Mn obtained from all four chemical fractions of the BCR-SE method was evaluated.

The Mn bound to the different chemical fractions was determined by flame and electrothermal atomic absorption spectrometry. The pH of the soil of the three mining areas was in the range of 6.2–6.8. The major fraction of Mn was found in the reducible fractions, whereas the organically bound form was lower for the three soil samples. The sequence of the chemical forms was in decreasing order: $Mn_{reducible} < Mn_{residual} < Mn_{oxidizable} < Mn_{acid\text{-}soluble}$ which indicates that the major form of Mn was in poorly available form.

INTRODUCTION

Coal mining and coal processing are of profound environmental concern due to the generation of large quantities of dust particles and mine spoil containing toxic elements dispersed in the dust and soils with potentially adverse health impact on nearby inhabitants of the mines. Open-throw coal mining results in huge quantities of dust and gas emissions containing metals and metalloids in very low quantities. When coal is combusted for energy production, as for the thermal power plants, the metal concentrations increase considerably (1). The waste from coal (ash) near power plants contains elevated levels of elements (As, Cr, Mn, V, Pb, and Zn) which can adversely influence the soil quality and flora and fauna of the area (2).

In this study, manganese (Mn) is selected because of its high exposure especially to miners and causes neurological disorders such as Parkinson's disease. Manganese is an essential trace element (at normal levels (2.0 to 5.0 mg/minimum daily allowance) and is required for normal physiological functions, especially related to the reproductive functions. A deficiency of Mn can cause skeletal abnormalities and irregular metabolism of carbohydrates and lipids.

Establishing the trace toxic elements found around thermal power plants due to coal burning for energy production can provide valuable information about possible contamination in the air and soil, as well as the surface and groundwater systems (3, 4). Availability of toxic elements depends on the surface characteristics of the coal particles, the chemical bonding forms, as well as the type and concentration of the solution used for extraction (5). Soil and water reservoirs are frequently contaminated with inorganic and organic pollutants causing adverse effects on food crops and plants (6).

Manganese is not found in free form, but in different chemical compounds together with carbonates, sulfides, phosphates, oxides, borates, and silicates (7). The metal accumulation in coal is due to degraded plant material and the soil. It has been reported (8) that burning of coal converts the metals and metalloids to less volatile or stable forms. On cooling, the volatilized metal and metalloid vapors settle onto the surface of the soil. Thus, these elements might be more mobile than in their original form in the coal samples.

The elements generally found in environmental samples are due to natural and anthropogenic sources and are in different chemical forms. For the chemical fractionation of Mn and other metals in soil, residual and fly ash, the BCR sequential extraction scheme is generally used and consists of four steps: acid-soluble, reducible, oxidizable, and residual. Manganese is found in three potential oxidation states in soil and fly ash: Mn(II), Mn(III), and Mn(IV). The most stable form is the divalent ion of Mn(II), whereas Mn(III) and Mn(IV) are stable only in solid form. (9 -11).

Corresponding author.
E-mail: tgkazi@yahoo.com
Tel: +92 22-2772065, 9213429
Fax: + 92 22-9213431

The extraction of the easily available/bioavailable fraction of metals in environmental solid samples requires mild neutral salt solutions of $NaNO_3$, KNO_3, $CaCl_2$, CH_3COONH_4 and EDTA, whereas water-soluble metals are in an immediately available form for plants. Thus, to obtain information about metals in their different chemical forms, the binding characteristics of the ingredients, and their possibility of transport, requires a multistage extraction method (12).

The availability of Mn in soil is controlled by its redox potential and the soil pH, where the lower pH/redox potential reduces its insoluble form and enhances its mobility. When the soil pH is > 6, Mn is most probably bound with organic matter, oxides, and silicates which reduces its solubility. The solubility and availability of Mn is, therefore, normally low at a high pH and with high organic matter content, whereas at low pH (acid soils) and a low quantity of organic matter the availability of Mn is high. At anaerobic and aerobic conditions at pH > 6 and below 5.5, the solubility of Mn is high (13).

This study was carried out at the coal mining area within the district of Jamshoro, Sindh, Pakistan, to assess the potential human exposure risks due to Mn in the surrounding soil. The soil samples were collected from three mining zones of the Lakhra power plant. The three-stage sequential extraction scheme was used. In addition, the determination of the water-soluble elements in these soil samples was carried out using the German Standard Method (DIN 38414-S4) (14).

EXPERIMENTAL

Instrumentation

The total concentration and fractionation of Mn with digests and using the BCR-SES method was performed using the AAnalyst™ 700 double beam flame atomic absorption spectrometer (FAAS) (PerkinElmer, Inc., Shelton, CT, USA), equipped with a pyrocoated graphite tube and integrated platform, and an AS-800 autosampler. Centrifugation was carried out using a Model 1465 centrifuge (speed range 0–6,000 rpm, timer 0–60 minutes, 220/50 HZ, Histam-R, Spain). Also used for the experimental work were an electric shaker (Gallenkamp, Germany), digital pH-meter (WTW Inolab pH 740 meter, Germany), digital conductivity meter (WTW Inolab EC 720 meter, Germany), and a muffle furnace. The instrumental operating parameters are listed in Table I.

Sampling

The samples were taken from the surface soil layer (0–25.0 cm), collected during 2017 from the three coal mining areas (n=20 each), air-dried at room temperature for about 8 days. Then they were screened through a Nylon 2 mm sieve (purchased at a local market), made into 10 composite samples from each site, and stored in polypropylene containers at ambient temperature until analysis.

BCR Sequential Extraction Method

For the modified BCR four-stage sequential extraction, different extracts and extraction settings were used (Table II). For the modified BCR-SE scheme, a higher concentration of reagent (20 mL of hydroxyl amine hydrochloride) was used for the reducible fraction of Mn.

For replicate analysis, three samples of the air-dried composite soil samples (collected from the Lakhra coal mining area) were used. For all extraction steps, blank experiments (without standards/samples) were carried out.

The samples in the flasks were shaken at 30 rpm with a mechanical shaker at 25–30°C (room temperature) which is higher than the temperature (20°C) generally used and reported in the literature (15). Owing to the temperature and climate of the study area, the weight of the soil samples and the quantity of the extracting solutions were reduced. However, the proportion of solid solution used was similar to what was reported in the literature (11). Information about the experimental procedure is accessible elsewhere (16).

The experimental and extraction steps used in this study are listed in Table II. For calculation of the Mn levels in the soil samples, duplicate soil samples from each site were heated in an oven at 100±5 °C until a stable weight was obtained. Thus, the obtained analytical value at each step was based on dry basis

TABLE I
Instrumental Parameters for Flame and Electrothermal Atomic Absorption Spectrometer for the Determination of Mn

	AAnalyst 800 Flame AAS Program Used			
Metal	Wavelength (nm)	Lamp Current (mA)	Bandpass (nm)	Air Acetylene Flow Rate (L min^{-1})
Mn	279.5	15	0.2	11:1

	AAnalyst 800 Furnace AAS Program Used			
Metal	Wavelength (nm)	Spectral Bandwidth (nm)	Lamp Current (mA)	Background Corrector
Mn	279.5	0.2	7	On

(mg kg^{-1} of the metals according to dry weight of soil).

The extraction of Mn was carried out in all four steps/chemical fractions using different reagents. It was, therefore, not possible to provide a calibration graph with a simple standard of Mn salt. For this purpose, the extractant after each step was evaporated at 80 °C on an electric hot plate until a semi-residual mass was obtained. The residual mass was diluted with 0.2 N HNO_3 and filtered through a #42 Whatman filter to obtain the same matrixes for both the standards and the samples.

Leaching Test (DIN 38414-S4)

The water-soluble fraction of the metals in the environmental solid samples was determined using the German Standard Method DIN 38414-S4. Leaching of Mn was performed by adding ultrapure water to duplicates of each composite soil sample at a ratio of (1:10), and were left standing for 16 hours at room temperature. Then, the samples were filtered to separate the residual soil from the extractant, then filtered through a prewashed membrane filter of pore size 0.45 µm. The pH values, electrical conductivities, and concentrations of the extracted Mn were measured by electrothermal atomic absorption spectrometry (ETAAS).

Quality Parameters

Due to the unavailability of a certified reference material for Mn in soil, the validity of the BCR sequential extraction method was assessed using three replicate subsamples of soil collected from the three mining areas, spiked with known standards at two concentration levels. The accuracy was further confirmed by analyzing triplicates of each composite soil sample. The recoveries for the spiked Mn were usually quantitative, whereas the extraction recoveries of Mn were found to be lower for the oxidizable fraction where somewhat low recoveries were obtained, but the difference was not significant ($p<0.05$). The percentage recovery of the spiked Mn in each fraction of BCR was in the range of 97.1–98.4%, indicating a non-significant difference ($p>0.05$) (see Table III). Furthermore, the accuracy of the sequential extraction of Mn obtained by the sum of its concentrations was found good and compared well with the total concentrations directly determined from the corresponding soil samples, also termed pseudo-total. The recovery(%) of Mn was calculated as:

$$\text{Recovery (\%)} = \frac{\Sigma \text{ of four fractions}}{\text{Pseudo-total contents}} \times 100$$

TABLE II
Chemical Reagents and Extraction Conditions for Optimized BCR-SES and Aqua Regia Digestion of Soil Samples

Steps		
1. Acid-soluble	20 mL of 0.11 M acetic acid was added to 0.5 g of air-dried IWS and CRM samples, shaken for 12-24 hours. The mixture was centrifuged to separate the extract from the residue.	Exchangeable, water and acid,- and acid soluble, (e.g., carbonates)
2. Reducible	20 mL of freshly prepared hydroxyl ammonium chloride, adjusted with nitric acid to pH 1.5, was added to the residue from Step 1, and the extraction performed as above.	Reducible (e.g., organic substance and sulfides)
3. Oxidizable	The residue from step 2 was treated twice with 5 mL 30% hydrogen peroxide, evaporated to near dryness, and then 25 mL of ammonium acetate (adjusted to pH 2 with nitric acid) was added and the extraction performed as above.	Oxidizable (e.g., organic substance and sulfides)
4. Residual	8 mL of aqua regia (HCl/HNO_3, 3:1) was added to residue obtained after the third step, and digested on a hot plate at 100 ºC as described below.	Remaining non-silicate-bound metals

RESULTS AND DISCUSSION

Mn Fractionation in the Soil Samples

The four-step BCR sequential extraction scheme provides the chemical forms of the metals, informs of their availability, mobilization, and transportation of Mn from different soil samples to the environment, especially into groundwater. For the present sequential extraction steps corresponding to soluble Mn in weak acid (acid-soluble) form, hydroxyl ammonium chloride was used as the extractant and termed as the reducible fraction, whereas the third chemical fraction was the oxidizable form.

Sequential extraction procedures provide useful information for risk assessment of the metals and to estimate the amount of metals mobilized under different environmental conditions (weakly acidic conditions: Step 1, reducing conditions: Step 2, and oxidizing conditions: Step 3). The different chemically bound forms or distribution

patterns of Mn are listed in Table IVa. It was observed that the major amount of Mn is stable and not extracted by water. However, a very small percentage (0.337 – 0.507%) of the total concentration of Mn was soluble in water (Table IVa).

The first fraction of BCR-SES (acid-soluble metals) in general has comparatively little concentration of metals and is determined by electrothermal atomic absorption spectrometry (ETAAS). For the acid-soluble fraction of Mn, a 0.11 M of CH_3COOH was used. The mild concentration of acid can dissolve the Mn bound with the carbonate compounds, which does not react or dissolve the Mn bound with alumino silicates, organic matter, Fe and Mn oxides (17).

The concentration of Mn in the acid soluble/carbonate fraction was in the range of 5.2 to 5.74% of total content in the different soil samples, which might be considered as the more mobile and bio-available form for plant uptake. The chemical fraction of the metals, which precipitate or co-precipitate with carbonate compounds, are easily extracted out with a mild concentration of acid. It was reported that metals found in this fraction bind loosely with the carbonate form and are easily available when environmental conditions (such as pH) change (18,19).

The highest amount of Mn (45.6 to 48.2% of total Mn) was observed for the reducible fraction. Thus, the Mn bound with the iron-Mn oxide lattice is liberated when the matrices of the environmental samples are treated at reducing environment by means of reducing agent hydroxyl ammonium chloride (20). It was reported that the amount of iron-Mn oxides is higher in sediment and soil samples, but less in solid samples enriched with organic matter (21).

The oxidizable fraction was found to be lower than the Mn bound with iron-manganese oxide in the soil samples collected from the coal mining areas. The % of Mn bound with organic matter of the oxidizable Mn corresponds to 7.26 to 8.38% of its total concentration in all three soil samples. The metals bound with the organic portion of the solid samples become available when treated with the oxidizing reagents. It can be stated that the metals are not easily available because they are bound with the humic substances and have, therefore, high molecular weight, and to liberate small amounts of metals requires a long time period (22). It was reported that the deprivation of metals in an oxidizing environment can be due to their decomposition in organic matter and releases them into the environment (23). It was also noted that the divalent metal ions, in comparison to monovalent ions, have elevated selectivity for compounds that are organic in nature.

The hydrogen peroxide in acid medium is mostly used for the third fraction (oxidizable) of the BCR-SES method. The residual fraction of Mn in the three composite soil samples is partitioned in the residual phase corresponding to 37.1 to 39% of total concentration. The

TABLE III
Standard Addition/Recovery for Mn Fractions in Real Soil Samples From PMDC Mining Areas of Lakhra Coal Field

Added Mn (mg/L)	Acid-soluble	(%)R[b]	Reducible	(%)R	Oxidizable	(%)R	Residual	(%)R
0.0	8.4±0.71[a]		110±6.53		16.0±1.02		84.0±4.4	
5.0	13.1±1.2	97.6	112.7±8.2	98.0	20.4±1.23	97.1	87.0±2.7	98.2
10.0	18.1±1.71	98.4	117.6±7.47	97.8	25.5±1.65	98.1	92.0±5.2	97.9

[a] Means of six replicates with standard deviations.
[b] (%)Recovery.

TABLE IVa
Fractionation of Mn in Soil Samples of Different Coal Mining Areas

Soil Sample/ Fractions	Water-soluble	Acid-soluble	Reducible	Oxidizable	Residual
S1 (mg/kg)	1.12±0.15	8.42±0.451	106± 7.65	16.0±1.12	82.4±6.74
% of Total	0.507	5.74	49.2	7.407	37.1
S2	2.2±0.12	27.6±1.76	240± 14.4	42.5± 1.21	191±16.8
% of Total	0.439	5.24	48.1	8.383	38.12
S3	0.98±0.028	16.1± 1.12	140±11.8	21.1±1.81	113±7.34
% of Total	0.337	5.5	48.2	7.26	38.9

TABLE IVb

Sample	∑ of Four Fractions	Pseudo-total	(%) Relative Errors
S1	217	221	1.81
S2	501	502	0.063
S3	290	291	0.371

S1= Pakistan Mineral Development Corporation.
S2= Irfan Coal Mine.
S3= Indus Coal Mine.

residual fraction is bound to a stable lattice structure in the environmental solid samples. The concentrations of the chemical fractions of Mn in the soil samples were found in decreasing order: Acid-soluble Mn > Oxidizable Mn > Residual Mn > Reducible Mn. The leachable fraction of Mn collectively with the other two fractions, acid-soluble and oxidizable fraction, was usually not found to be very elevated in the sediment and soil samples. The comparison of the sum of concentrations of Mn in all four fractions of the BCR procedure to the total concentrations obtained after digestion with the acid mixture is shown in Table IVb.

Another significant feature of the fractionation data is the ability to obtain the percentage of the labile concentration of the metals in the environmental solid samples (soil and sediment). It is equivalent to the sum from fractions 1–3, the total concentrations obtained from all fractions of BCR-SES (including the residual concentration). The resulting data indicated that the labile fraction of Mn in the soil samples was > 60%. It was reported that in general if the percent values obtained from the sum of the first three fractions are higher than the residual concentrations, larger adverse effects occur that contaminate the water bodies and bio-accumulate in plants (24).

Elevated levels of metals available/mobile as extracted in mild extractants might easily enter into the soil to contaminate agricultural systems. The mobile/bio-available contents of Mn in the soil samples are particularly susceptible to conditions such as wetness, content of organic material, biological activity, pH/acidity, etc. The soluble fraction of Mn in soil might be restricted by its pH and redox potential, whereas at lower values of both factors (pH and redox potential) it helps to enhance the mobility of Mn.

When at higher pH (pH > 6.0), the Mn solubility/bio-availability is decreased, which might be due to the association of Mn bound with oxides, silicates, and organic matter. At lower levels of organic matter and higher pH of the environmental solid samples, the availability/solubility of Mn is lowered. However, at lower pH (acidic soil), the solubility of Mn in an aqueous medium is higher. This study found that at anaerobic conditions of soil/sediment samples at pH >6 (while aerobic conditions at pH <5.5), the availability/solubility of Mn becomes enhanced at the pH above 6 as well as in aerobic conditions at the pH below 5.5 (25).

To evaluate the available/bio-available concentration of metals in different environmental solid samples, mild extractants are used such as H_2O, $CaCl_2$, NH_4NO_3, $NaNO_3$, and EDTA as single extractant. Whereas for metals and metalloids bound to different chemical lattices of environmental samples, different sequential extraction schemes are selected. Although Mn is an essential trace element and necessary for different physiological systems in trace quantities, high intake/exposure becomes a negative and can occur through the contamination of drinking water, food crops, as well as due to burning fossil fuels.

CONCLUSION

The data obtained in this study indicates that the Mn concentration in all soil samples from the three different locations of the coal mining areas of the Lakhra coal fields were found in stable form and only <1% of the total concentration was immediately available to plants and the neighboring inhabitants of the area. The highest concentration of Mn was found in the reducible fraction and showed an association with soil pH. The metal can become bio-available to plants with a change in the redox or pH conditions of the soil. In coal mining areas, the Mn levels must be monitored to protect man and the environment.

Received April 2, 2018.

REFERENCES

1. R.E. Masto, L.C. Ram, J. George, V.A. Selvi, A.K. Sinha, S. K Verma, T.K. Rout, and Priya Darshini, Toxicol. Environ. Chem. 93, 223 (2010).
2. L. Bityukova, A. Shogenova, and M. Birke, Environm. Geochem.and Health 22, 2 (2000).
3. R.B. Finkelman, W. Orem, V. Castranova, C.A. Tatu, H.E. Belkin, B.Zheng, and A.L.Bates, Internatl. J. Coal Geology 50(1-4), 425 (2002).
4. Y. Tang, C. Chang, Y. Zhang, and W. Li, Energy Exploration & Exploitation 27(2), 143 (2009).
5. Kalembkiewicz, J., Sitarz-Palczak, E., and Zapała, L. Microchem. J. 90(1), 37 (2008).
6. George, Joshy, Reginald E. Masto, Lal C. Ram, Tarit B. Das, Tofan K. Rout, and Mahesh Mohan. Archives of Environmental Contamination and Toxicology, 68(3), 451 (2015).
7. Gerber, G. B., Leonard, A., and Hantson, P. Critical Reviews in Oncology/Hematology 42(1), 25 (2002).
8. Kalembkiewicz, J., Sitarz-Palczak, E., and Zapała, L., Microchem. J. 90(1), 37 (2008).
9. Gerber, G.B., Leonard, and A. Hantson, P., Critical Reviews in Oncology/Hematology 42, 25 (2002).
10. Howe, P., Malcolm, H. and Dobson, Environmental Aspects, World Health Organization, Geneva, Switzerland, pp. 63 (2004).
11. Grygo-Szymanko, Emilia, Anna Tobiasz, and Stanislaw Walas, "Speciation analysis and fractionation of manganese: A review", TrAC Trends in Analytical Chemistry (2016).

12. Howe, P., Malcolm, H., and Dobson, S. environmental aspects (No. 63). World Health Organization (2004).
13. Kabata-Pendias, A., Trace elements in soils and plants, CRC Press (2010).
14. DIN 38414-S4. German standard methods for the examination of water, wastewater and sludge. Group S (sludge and sediments). Determination of leachability by water (S4). Deutsches Institut für Normung, Berlin, Germany (1984).
15. Pueyo, M., Rauret, G., Lück, D., Yli-Halla, M., Muntau, H., Quevauviller, P., and López Sánchez, J. F., Journal of Environmental Monitoring 3(2), 243 (2001).
16. Kazi, T. G., Jamali, M. K., Kazi, G. H., Arain, M. B., Afridi, H. I., and Siddiqui, Anal. and Bio-anal. Chem. 383(2), 297 (2005).
17. Rauret, G., López-Sánchez, J. F., Sahuquillo, A., Barahona, E., Lachica, M., Ure, A. M., and Yli-Halla, M., J. of Environm. Monitoring 2(3), 228 (2000).
18. Ali, J., Kazi, T. G., Baig, J. A., Afridi, H. I., Arain, M. S., Brahman, K. D., and Panhwar, A. H., Environmental Science and Pollution Research 22(11), 8559 (2015).
19. Emmerson, R. H. C., Birkett, J. W., Scrimshaw, M., and Lester, J. N., Science of the Total Environment 254(1), 75 (2000).
20. García-Miragaya, J., and Sosa, A. M., Water, Air, and Soil Pollution, 77(1-2), 141 (1994).
21. Davidson, C. M., Wilson, L. E., and Ure, A. M., J. of Anal. Chem. 363(1), 134 (1999).
22. Sutherland, R. A., and Tack, F. M., Anal. Chim. Acta 454(2), 249 (2002).
23. Michalke, K. and Fernsebner, J., Trace Elem. Med. Biol. 28, 106 (2014).
24. P. Anschutz, K. Dedieu, F. Desmazes, and G. Chaillou, Chem. Geol. 218, 265 (2005).
25. Sutcu, E.C., Karayigit, A. I., Internatl. J. of Coal Geol. 144–145, 111 (2015).

The Titan MPS™ microwave is the safe, cost-effective, easy-to-use sample preparation system – the go-to platform for pressure digestion of a broad range of samples before inorganic analysis. But what really sets it apart is everything else you get with it: It's backed by PerkinElmer, the go-to resource and one-stop shop for all things atomic spectroscopy, so you can access the instruments, consumables, informatics, and expertise you need to optimize your research and your business. The Titan MPS sample preparation system: It's the microwave that's so much more.

www.perkinelmer.com/titanmps

PerkinElmer, Inc.
710 Bridgeport Avenue
Shelton, CT 06484-4794 USA
Phone: (800) 762-4000 or
(+1) 203-925-4602
www.perkinelmer.com

013948_06

PerkinElmer®
For the Better